In memory of T. A. Stephenson

Reactions of Tetra-μ-carboxylato-diruthenium(II,II) Compounds. *X*-Ray Crystal Structures of $Ru_2(\mu\text{-}O_2CCF_3)_4(thf)_2$, $Ru_2(\mu\text{-}O_2CR)_4(NO)_2$ (R = Et or CF_3), and $\{Na_3[Ru_2(\mu\text{-}O_2CO)_4]\cdot 6H_2O\}_n$†

Alan J. Lindsay and Geoffrey Wilkinson*
Chemistry Department, Imperial College, London SW7 2AY
Majid Motevalli and Michael B. Hursthouse*
Chemistry Department, Queen Mary College, London E1 4NS

Improved procedures for the synthesis of the diruthenium(II) carboxylates, $Ru_2(\mu\text{-}O_2CR)_4L_2$, and substitutions of either the bridged carboxylate or axial ligands (L) are described. Among new bridged compounds are the trifluoroacetate, $Ru_2(\mu\text{-}O_2CCF_3)_4$, the carbonate, $\{Na_3[Ru_2(\mu\text{-}O_2CO)_4]\cdot 6H_2O\}_n$, and the triazenide, $Ru_2(\mu\text{-}N_3Ph_2)_4$; adducts of the triazenide include the nitrosyl, $Ru_2(\mu\text{-}N_3Ph_2)_4(NO)_2$, the isocyanide, $Ru_2(\mu\text{-}N_3Ph_2)_4(Bu^tNC)$, and the carbonyl $Ru_2(\mu\text{-}N_3Ph_2)_4(CO)_2$. Reactions of the carboxylates with donors such as isocyanides, pyridine (py), phosphines, or CO leads in some cases to bridge cleavage and products such as *trans*-$Ru(O_2CR)_2(py)_4$ or $Ru(O_2CR)_2(PPh_3)_2$ (R = Me or CF_3), while the reactions with NO yield the diamagnetic adducts $Ru_2(\mu\text{-}O_2CR)_4(NO)_2$. Infrared, n.m.r., e.s.r., and electronic spectra are recorded together with cyclic voltammetric studies. The *X*-ray crystal structures of the dimers $Ru_2(\mu\text{-}O_2CCF_3)_4(thf)_2$ (thf = tetrahydrofuran) and $Ru_2(\mu\text{-}O_2CR)_4(NO)_2$ (R = Et or CF_3), and the polymer $\{Na_3[Ru_2(\mu\text{-}O_2CO)_4]\cdot 6H_2O\}_n$ are reported.

Binuclear carboxylato compounds of type $M_2(\mu\text{-}O_2CR)_4L_2$ (M = Cr, Mo, W, or Rh; R = alkyl or aryl) have been used for the synthesis of diverse co-ordination and organometallic compounds.[1-4] The main types of reaction include (*a*) those in which the $M_2(\mu\text{-}O_2CR)_4$ unit is retained; (*b*) those where substitution of some or all of the carboxylate ligands occurs (with or without redox processes at the M_2^{4+} core); and (*c*) those where the binuclear unit is cleaved.

We recently described the first synthesis of several compounds of the type $Ru_2(\mu\text{-}O_2CR)_4$ (R = H, Me, CH_2Cl, Et, or Ph),[5] although the mixed-valence Ru_2^{5+} core polymeric species $[Ru_2(\mu\text{-}O_2CMe)_4Cl]_n$,[6] prepared by T. A. Stephenson, has long been known and used in other syntheses.[1]

We now describe several complexes obtained by reaction of $Ru_2(\mu\text{-}O_2CMe)_4$ with potentially bridging anionic ligands, donor ligands, and oxidising agents, and some reactions thereof. Analytical and other data for the new compounds are given in Table 1, spectroscopic data in Tables 2 and 3; potentials given in the text are all *versus* the saturated calomel electrode at which ferrocene is oxidised at +0.34 V.

Results and Discussion

Reaction of $Ru_2(\mu\text{-}O_2CR)_4$ *with Potentially Bridging Anionic Ligands.*—(a) *Carboxylate exchange reactions; the trifluoroacetate system.* The carboxylates $Ru_2(\mu\text{-}O_2CR)_4$ (R = H, Me, Et, Ph, or CH_2Cl) were originally obtained on reaction of the appropriate alkali-metal carboxylate salt with the reduced 'blue solution' from ruthenium trichloride in methanol.[5] Both the yield and the range of these compounds can be improved by exchange reactions.

The reaction of Li or Na carboxylates in methanol with $Ru_2(\mu\text{-}O_2CH)_4$ [the carboxylate obtained in highest yield (63%) by the reduced 'blue solution' method] leads to the fast (less than 30 min) and efficient (up to 92% yield) formation of the appropriate carboxylate $Ru_2(\mu\text{-}O_2CR)_4$ (R = Me, Et, Ph, or CH_2Cl). The method fails for the trifluoroacetate and prolonged reflux of $Ru_2(\mu\text{-}O_2CR)_4$ (R = H or Me) in either methanol or water in the presence of 12 equivalents of $Na[O_2CCF_3]$ leads only to the isolation of starting material.

However, interaction of 12 equivalents of $Ag[O_2CCF_3]$ with $Ru_2(\mu\text{-}O_2CMe)_4$ in refluxing methanol gives a red-orange product analysing (Table 1) as $Ru_2(O_2CMe)_4(O_2CCF_3)$. Solid and solution magnetic susceptibility measurements give $\mu_{eff.}$ = 2.9 B.M. per Ru. The characteristic e.s.r. ($S = \frac{3}{2}$) spectrum for a Ru_2^{5+} core ($g_\perp = g_\parallel = 2.1 \pm 0.1$) in ethanol glass at 77 K corresponds to three unpaired electrons per Ru_2 unit, consistent with the oxidation by Ag^+ of the Ru_2^{4+} core. These magnetic and spectroscopic features are characteristic of other Ru_2^{5+} core complexes such as $[Ru_2(\mu\text{-}O_2CPr^n)_4Cl]_n$,[7] which are believed to possess a $\sigma^2\pi^4\delta^2\pi^{*2}\delta^{*1}$ electronic configuration.

The mull i.r. spectrum (Table 2) shows intense bands at 1 654 and 1 441 cm^{-1} attributable to $\nu_{asym}(CO_2)$ in $O_2CCF_3^-$ and O_2CMe^-, respectively, and weaker bands at 1 465 and 1 405 cm^{-1} due to $\nu_{sym}(CO_2)$ in $O_2CCF_3^-$ and O_2CMe^- respectively. The relatively large $\Delta\nu(\nu_{asym} - \nu_{sym})$ for the $O_2CCF_3^-$ bands is compatible with symmetric bridging co-ordination;[8] the small $\Delta\nu$ for the O_2CMe^- bands is not a general characteristic of symmetric bridge co-ordination but is a peculiarity of the $[Ru_2(\mu\text{-}O_2CR)_4X]_n$ system.[6]

The formulation $[Ru_2(\mu\text{-}O_2CMe)_4(O_2CCF_3)]_n$ is confirmed by cyclic voltammetric studies (Figure 1) in the presence and absence of NBu^n_4Cl. In the absence of an excess of Cl^- there are three reduction waves at *ca.* +0.05, −0.14, and −1.83 V; the

† Tetra-μ-trifluoroacetato-diruthenium(II,II)–tetrahydrofuran(1/2), tetra-μ-propionato- and tetra-μ-trifluoroacetato-bis[nitrosyl-ruthenium] and trisodium tetra-μ-carbonato-diruthenate(II,III) hexahydrate respectively

Supplementary data available: see Instructions for Authors, *J. Chem. Soc., Dalton Trans.*, 1987, Issue 1, pp. xvii—xx.

Non-S.I. units employed: B.M. = 0.927 × 10^{-23} A m^2, atm = 101 325 N m^{-2}, mmHg = (101 325/760) N m^{-2}.

first two waves [Figure 1(*a*)] represent the two-step reduction process previously identified for $[Ru_2(\mu\text{-}O_2CPr^n)_4Cl]_n$ in both 0.1 mol dm^{-3} $NBu^n_4ClO_4$–dichloromethane[7] and acetonitrile,[9] while the irreversible reduction at a more negative potential is also a recognised feature of the electrochemistry of $[Ru_2(\mu\text{-}O_2CR)_4X]_n$ in acetonitrile.[9] In the presence of a ten-fold excess of NBu^n_4Cl the situation is greatly simplified [Figure 1(*b*)], showing a single reversible one-electron reduction at −0.45 V attributable to the $Ru_2(\mu\text{-}O_2CMe)_4Cl_2^{1-/2-}$ redox couple.[5]

This electrochemistry agrees with the established reduction mechanism for $[Ru_2(\mu\text{-}O_2CPr^n)_4Cl]_n$[7,9] [equation (1)].

$$[Ru_2(\mu\text{-}O_2CMe)_4]^+ + nX^- \overset{\text{slow}}{\rightleftharpoons} [Ru_2(\mu\text{-}O_2CMe)_4X_n]^{(n-1)-}$$
$$E_{\frac{1}{2}} +0.05\text{ V} \Big\| +e^- \qquad +e^- \Big\| \begin{matrix} X = O_2CCF_3^-, E_{\frac{1}{2}} -0.14\text{ V} \\ X = Cl^-, E_{\frac{1}{2}} -0.45\text{ V} \end{matrix} \quad (1)$$
$$Ru_2(\mu\text{-}O_2CMe)_4 \qquad [Ru_2(\mu\text{-}O_2CMe)_4X_n]^{n-}$$

On refluxing $Ru_2(\mu\text{-}O_2CMe)_4$ in a $EtCO_2H$–$(EtCO)_2O$ mixture the polymeric complex $[Ru_2(\mu\text{-}O_2CEt)_4(O_2CEt)]_n$ is formed essentially quantitatively. This compound is analogous to the previously characterised acetate $[Ru_2(\mu\text{-}O_2CMe)_4(O_2CMe)]_n$.[10] The formal oxidation of the Ru^{II}_2 core to that of a $Ru^{II}Ru^{III}$ core under these reaction conditions is not surprising given the facility of the Ru^{II}_2–$Ru^{II}Ru^{III}$ redox couple in these compounds.[5]

However, when a CF_3CO_2H–$(CF_3CO)_2O$ mixture containing $Ru_2(\mu\text{-}O_2CMe)_4$ and excess $Na[O_2CCF_3]$ is held under prolonged reflux only ligand replacement occurs and the product, recrystallised from tetrahydrofuran (thf)–n-hexane, is the red-orange air-stable trifluoroacetate, $Ru_2(\mu\text{-}O_2CCF_3)_4(thf)_2$. On heating *in vacuo* at 150 °C this gives $Ru_2(\mu\text{-}O_2CCF_3)_4$. In common with other Ru^{II}_2 tetracarboxylates[5] the mass spectrum of the weak thf adduct and the non-solvated complex are identical in the high mass region, both having the same parent ion, $[Ru_2(O_2CCF_3)_4]^+$, at m/e = 654. The i.r. spectra of both compounds (Table 2) show an intense $\nu_{asym}(CO_2)$ band at *ca.* 1 635 cm^{-1} and a weak $\nu_{sym}(CO_2)$ band at *ca.* 1 460 cm^{-1}. The relatively large $\Delta\nu$ indicates symmetric bridging[8] as confirmed by *X*-ray crystallography (see below).

The electronic spectrum of $Ru_2(\mu\text{-}O_2CCF_3)_4(thf)_2$ is qualitatively the same as that of other members of the series $Ru_2(\mu\text{-}O_2CR)_4(thf)_2$[5] in having a single low-intensity band ($\lambda_{max.}$ 456 nm, $\varepsilon_{max.}$ 950 dm^3 mol^{-1} cm^{-1}) in thf. Bands in this region ($\lambda_{max.}$ 438—448 nm) have been ascribed to O(π) – MM(π*) transitions where the 'O(π)' orbital is mainly Ru–O bonding in character, but with an appreciable Ru–Ru π-bonding contribution as well.[11]

Table 1. Analytical data for ruthenium complexes

Complex	Analysis (%)* C	H	Other
$[Ru_2(\mu\text{-}O_2CMe)_4(O_2CCF_3)]_n$	21.9 (21.8)	2.2 (2.2)	F 9.8 (10.3)
$[Ru_2(\mu\text{-}O_2CEt)_4(O_2CEt)]_n$	32.1 (31.8)	4.4 (4.4)	O 27.4 (28.2)
$[Ru_2(\mu\text{-}O_2CCF_3)_4(O_2CCF_3)]_n$	15.7 (15.4)	— (—)	F 37.2 (36.9) O 20.9 (20.7)
$Ru_2(\mu\text{-}O_2CCF_3)_4(thf)_2$	24.5 (24.1)	2.1 (2.0)	F 27.4 (28.6) O 20.3 (20.1)
$Ru_2(\mu\text{-}O_2CCF_3)_4$	14.9 (14.7)	— (—)	F 34.2 (34.9) O 20.6 (19.6)
$\{K_3[Ru_2(\mu\text{-}O_2CO)_4]\cdot 6H_2O\}_n$	7.5 (7.2)	2.0 (1.8)	O 42.6 (43.2) K 17.0 (17.5)
$\{Na_3[Ru_2(\mu\text{-}O_2CO)_4]\cdot 6H_2O\}_n$	7.4 (7.8)	2.2 (1.9)	O 45.7 (46.5) Na 10.6 (11.2)
$Ru_2(\mu\text{-}O_2CMe)_4(NO)_2$	19.3 (19.3)	2.2 (2.4)	N 5.6 (5.6)
$Ru_2(\mu\text{-}O_2CEt)_4(NO)_2$	26.3 (26.0)	3.6 (3.6)	N 4.9 (5.1)
$Ru_2(\mu\text{-}O_2CPh)_4(NO)_2$	44.5 (45.0)	2.7 (2.7)	N 3.6 (3.8)
$Ru_2(\mu\text{-}O_2CCF_3)_4(NO)_2$	13.4 (13.5)	— (—)	N 4.1 (3.9) F 31.3 (31.9)
cis-$Ru(O_2CCF_3)_2(Bu^tNC)_4$	42.8 (43.7)	5.3 (5.5)	N 8.2 (8.5)
fac-$Ru(O_2CCF_3)_2(CO)_3(thf)$	26.8 (27.3)	1.4 (1.7)	F 22.8 (23.6)
$[Ru(O_2CCF_3)(MeCN)_5]O_2CCF_3$	31.6 (31.6)	2.7 (2.8)	N 12.8 (13.2) F 20.1 (20.7)
trans-$Ru(O_2CCF_3)_2(py)_4$	44.6 (44.8)	3.1 (3.1)	N 8.7 (8.7) F 17.5 (17.7)
$Ru_2(\mu\text{-}N_3Ph_2)_4$	59.0 (58.4)	4.2 (4.1)	N 17.2 (17.1)
$Ru_2(\mu\text{-}N_3Ph_2)_4(NO)_2$	54.2 (55.1)	3.8 (3.8)	N 18.3 (18.7)
$Ru_2(\mu\text{-}N_3Ph_2)_4(Bu^tNC)$	59.8 (59.5)	4.7 (4.6)	N 16.8 (17.0)
$Ru_2(\mu\text{-}N_3Ph_2)_4(CO)_2$	58.1 (57.6)	3.9 (3.9)	N 16.1 (16.1) O 2.8 (3.1)

* Calculated values in parentheses.

Table 2. Selected infrared data (cm^{-1}) for ruthenium carboxylates

Complex	$\nu_{asym}(CO_2)$	$\nu_{sym}(CO_2)$	$\Delta\nu(\nu_{asym} - \nu_{sym})$	Others[a]
$[Ru_2(\mu\text{-}O_2CMe)_4(O_2CCF_3)]_n$	1 654, 1 441	1 465, 1 405	189, 36	
$[Ru_2(\mu\text{-}O_2CEt)_4(O_2CEt)]_n$	1 530, 1 470	1 430, 1 410	120, 40	
$[Ru_2(\mu\text{-}O_2CCF_3)_4(O_2CCF_3)]_n$	1 620, 1 539	1 471, 1 462	*ca.* 150, 70[b]	
$Ru_2(\mu\text{-}O_2CCF_3)_4(thf)_2$	1 643	1 462	181	
$Ru_2(\mu\text{-}O_2CCF_3)_4$	1 624	1 457	167	
$Ru_2(\mu\text{-}O_2CMe)_4(NO)_2$	1 582	1 442	140	ν(NO) 1 756
$Ru_2(\mu\text{-}O_2CEt)_4(NO)_2$	1 576	1 430	146	ν(NO) 1 722, 1 748 (1 745)[c]
$Ru_2(\mu\text{-}O_2CPh)_4(NO)_2$	1 553	1 416	137	ν(NO) 1 746
$Ru_2(\mu\text{-}O_2CCF_3)_4(NO)_2$	1 660	1 465	195	ν(NO) 1 800 (1 805)[c]
cis-$Ru(O_2CCF_3)_2(Bu^tNC)_4$	1 715	1 405	310	ν(CN) 2 225, 2 175, 2 150, 2 080 (2 222, 2 176, 2 145, 2 070)[d]
fac-$Ru(O_2CCF_3)_2(CO)_3(thf)$	1 700	1 410	290	ν(CO) 2 085, 2 020, 1 985 (2 085, 2 018, 1 990)[d]
$[Ru(O_2CCF_3)(MeCN)_5]O_2CCF_3$	1 720, 1 695	1 412, 1 430	308, 265	ν(CN) 2 295
trans-$Ru(O_2CCF_3)_2(py)_4$	1 700	1 410	290	

[a] Solution values are in given parentheses. [b] Average Δν values are given since we cannot differentiate between the two $\nu_{sym}(CO_2)$ values. [c] In hexane. [d] In CH_2Cl_2.

Table 3. ^1H and ^{19}F N.m.r. data for ruthenium compounds

Complex	$\delta(^1H)^a$	$\delta(^{19}F)^a$
$Ru_2(\mu\text{-}O_2CEt)_4(NO)_2$[b]	1.06(t), CH_3, $^3J_{HH}$ 7.6 Hz; 2.42(q), CH_2, $^3J_{HH}$ 7.6 Hz	
$Ru_2(\mu\text{-}O_2CCF_3)_4(NO)_2$[b]		−74.5(s), CF_3
cis-$Ru(O_2CCF_3)_2(Bu^tNC)_4$[c]	1.05(s), CH_3; 1.14(s), CH_3	−76.2(s), CF_3
fac-$Ru(O_2CCF_3)_2(CO)_3(thf)$[d]	2.06(m), CH_2; 4.06(m), OCH_2	−75.2(s), CF_3
$Ru(O_2CCF_3)_2(PPh_3)_2$[d,e]	6.7—7.4(m), Ph	−77.0(s), CF_3
$[Ru(O_2CCF_3)(MeCN)_5]O_2CCF_3$[f]	2.31(s), CH_3; 2.49(s), CH_3	−72.6(s), CF_3; −72.7(s), CF_3
trans-$Ru(O_2CMe)_2(py)_4$[b]	8.54(d), α; 7.55(t), β; 7.04(t), γ; 1.84(s), CH_3	
trans-$Ru(O_2CCF_3)_2(py)_4$[b]	8.44(d), α; 7.68(t), β; 7.17(t), γ	−74.0(s), CF_3
$Ru_2(\mu\text{-}N_3Ph_2)_4$[d,e]	7.13(d), α; 7.66(t), β; 6.56(t), γ	
$Ru_2(\mu\text{-}N_3Ph_2)_4(NO)_2$[b]	7.13(s), Ph	
$Ru_2(\mu\text{-}N_3Ph_2)_4(Bu^tNC)$[b]	6.5—7.5(m), Ph; 1.03(s), CH_3	
$Ru_2(\mu\text{-}N_3Ph_2)_4(CO)_2$[b]	6.9—7.3(m), Ph	

[a] s = Singlet, d = doublet, t = triplet, q = quartet, m = multiplet; $\delta(^1H)$ in p.p.m. relative to $SiMe_4$; $\delta(^{19}F)$ in p.p.m. relative to $CFCl_3$; at 308 K unless otherwise stated. [b] In $CDCl_3$. [c] In $[^2H_8]$ toluene. [d] In CD_2Cl_2. [e] Between 193 and 308 K. [f] In CD_3CN.

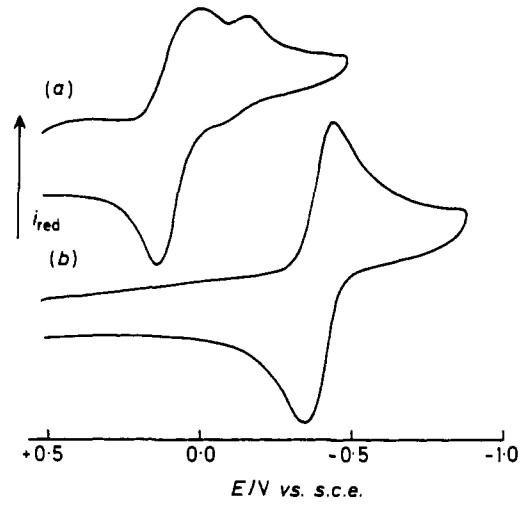

Figure 1. Cyclic voltammograms in 0.2 mol dm^{-3} $NBu^n_4PF_6$–MeCN; potential sweep rate 100 mV s^{-1}. (*a*) $[Ru_2(\mu\text{-}O_2CMe_4)(O_2CCF_3)]_n$, (*b*) in the presence of a 10-fold excess of NBu^n_4Cl

Solid and solution magnetic susceptibilities of $Ru_2(\mu\text{-}O_2CCF_3)_4(thf)_2$ correspond to $\mu_{eff.} = 2.1$ B.M. per Ru implying two unpaired electrons per binuclear unit; this agrees with values for the other ruthenium carboxylates[5] and for $Ru_2(\mu\text{-mhp})_4{\cdot}CH_2Cl_2$ (Hmhp = 2-hydroxy-6-methylpyridine) (electronic configuration $\sigma^2\pi^4\delta^2\delta^{*1}\pi^{*3}$),[12] as well as the theoretical predictions of Norman *et al.*[11] for $Ru_2(\mu\text{-}O_2CH)_4$ (electronic configuration $\sigma^2\pi^4\delta^2\pi^{*3}\delta^{*1}$). The absence of an e.s.r. spectrum for these paramagnetic systems has been tentatively attributed to a large zero-field splitting arising from strong magnetic dipole–dipole interaction between the two unpaired electrons in the assumed triplet ground state.[5]

Table 4. Cyclic voltammetry of $Ru_2(\mu\text{-}O_2CCF_3)_4$

Solvent	$E_{\frac{1}{2}}/V^a$ Ru^{II}_2–$Ru^{II}Ru^{III}$	$E_{\frac{1}{2}}/V^a$ Ru^{II}_2–$Ru^{II}Ru^{I}$
CH_2Cl_2[b]	*+1.17* (+0.53)[c]	(−0.76, −1.25)
Acetone[b]	[+1.03]	[−0.99]
Tetrahydrofuran[b]	—	*−1.15*

[a] Values in *italic* indicate a reversible redox couple; parentheses ( ) indicate an irreversible redox couple; parentheses [ ] indicate a partially reversible redox couple, *i.e.* in cyclic voltammetry i_p (forward) increases towards unity with increasing scan rate, consistent with slow reaction of the electrode product following reversible charge transfer: all $E_{\frac{1}{2}}$ values are referenced with respect to a saturated calomel electrode at which ferrocene is oxidised at +0.34 V. [b] Electrolyte solution contains 0.2 mol dm^{-3} $NBu^n_4PF_6$. [c] Solution contains a 10-fold excess of NBu^n_4Cl.

Cyclic voltammetric studies on $Ru_2(\mu\text{-}O_2CCF_3)_4$ (Table 4) indicate that the redox processes, unlike those of other Ru^{II}_2 carboxylates, are markedly solvent dependent. In CH_2Cl_2, a solvent of poor co-ordinating ability, $Ru_2(\mu\text{-}O_2CCF_3)_4$ undergoes a reversible one-electron oxidation at +1.17 V and two irreversible reductions at *ca.* −0.76 and −1.25 V respectively. In contrast, in better donor solvents the oxidation becomes either less reversible or absent within the solvent limit. At the same time the one-electron reduction process becomes more reversible; the process in acetone is partially reversible while that in thf is fully reversible.

The relative destabilisation of the higher $Ru^{II}Ru^{III}$ oxidation state of the $[Ru_2(\mu\text{-}O_2CCF_3)_4]^+$ core in thf and Me_2CO with respect to CH_2Cl_2 probably reflects the greater nucleophilicity and co-ordinating ability of these solvents towards the electron-deficient bimetallic core, which may ultimately be cleaved to yield monomers. The difference in oxidation potential of $Ru_2(\mu\text{-}O_2CCF_3)_4$ in CH_2Cl_2 and Me_2CO is attributable to the much weaker donor ability of the former over the latter. The stronger the interaction between the axial donor group and the ruthenium in $Ru_2(\mu\text{-}O_2CCF_3)_4$ the easier is the oxidation.[5,13]

The complex $Ru_2(\mu\text{-}O_2CCF_3)_4(Me_2CO)_2$ shows a considerably higher oxidation potential, +1.03 V, than $Ru_2(\mu\text{-}O_2CMe)_4(thf)_2$, −0.05 V, because of the strong electron-withdrawing properties of the CF_3 groups compared with the electron-donating nature of the Me groups. The effect of substituting axial Me_2CO for thf on the redox potential is expected to be negligible.[14]

The potential shift for the reduction of $Ru_2(\mu\text{-}O_2CR)_4L_2$ may be taken as a general measure of their acidity towards adduct formation.[13] With a strong electron-withdrawing group (R = CF_3, L = thf), the lower oxidation states are stabilised to such an extent that the Ru^{II}_2–$Ru^{II}Ru^{I}$ redox couple is fully reversible while no oxidation process can be observed before the onset of the anodic potential limit of thf. The opposite occurs with an electron-donating group (R = Me, L = thf) present, since a fully reversible oxidation and no reduction has been found.[5]

Whereas the reductions of $Ru_2(\mu\text{-}O_2CCF_3)_4$ in thf and Me_2CO appear to be similar, that in CH_2Cl_2 differs in that it features two irreversible electron transfers. The origin of the difference is not clear though doubtless the destabilisation of the reduced species in CH_2Cl_2, over thf or Me_2CO, is related to the non-co-ordinating nature of the solvent.

A profound change in both the colour (orange to cherry red) and the oxidation potential of a CH_2Cl_2 solution of $Ru_2(\mu\text{-}O_2CCF_3)_4$ is observed on adding a 10-fold excess of NBu^n_4Cl, due to the formation of $[Ru_2(\mu\text{-}O_2CCF_3)_4Cl_2]^{2-}$, which undergoes a single irreversible one-electron oxidation (reduction not observed) at a potential considerably more

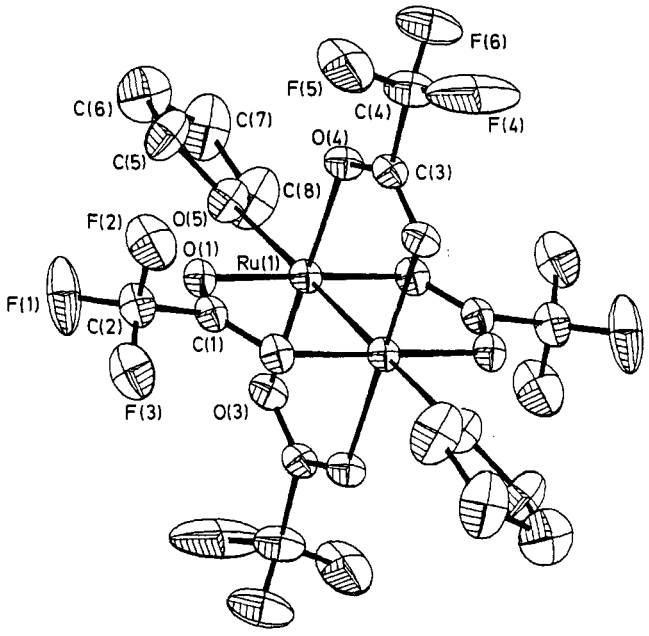

Figure 2. The structure of $Ru_2(\mu\text{-}O_2CCF_3)_4(thf)_2$

negative, *ca.* 0.64 V, than its neutral precursor. A similar change was previously noted for $Ru_2(\mu\text{-}O_2CMe)_4$ in the presence of excess Cl^-,[5] though here the redox couple remained reversible.

An even greater change in the electrochemical behaviour of $Ru_2(\mu\text{-}O_2CCF_3)_4$ is effected by using 0.2 mol dm^{-3}, $NBu^n_4PF_6$–acetonitrile as the electrolyte solution. The irreversible one-electron reduction at −0.97 V initially observed is completely lost within 5 min of dissolution and no further redox processes are observed upon subsequent cathodic scans.

The anodic region is considerably more complicated. The variation in peak current with time for the five observable processes suggests at least five redox active species in solution over the time-scale involved. The largest initial oxidation wave, at +1.32 V, in conjunction with the reduction at −0.97 V may represent the electrochemical behaviour of the transient species $Ru_2(\mu\text{-}O_2CCF_3)_4(MeCN)_2$. Within 90 s this oxidation wave is lost and replaced by new waves at +0.67, +0.94, +1.46, and +1.74 V accompanied by a change in colour from red-orange to yellow-orange. At this point the predominant electroactive species is represented by the wave at +0.67 V. The solution gradually becomes paler and after 10 min the wave at +1.74 V disappears. At the same time the waves at +0.94 and +1.46 V intensify at the expense of the wave at +0.67 V with the former greatly predominating over the latter.

After 17 h the virtually colourless solution shows only the two waves (at +0.94 and +1.46 V) with the intensities now reversed. Finally, after 40 h, and with no perceptible change in colour, the solution shows only one electroactive species at +1.46 V.

Electrochemical studies in 0.2 mol dm^{-3}, $NBu^n_4PF_6$–MeCN on $[Ru^{II}(O_2CCF_3)(MeCN)_5]O_2CCF_3$ [which was isolated upon reaction of $Ru_2(\mu\text{-}O_2CCF_3)_4$ with MeCN as an air-stable white solid, see below], indicate that this and the above final electroactive species are the same.

The slowness of the reaction converting the species associated with the +0.94 V wave into $[Ru(O_2CCF_3)(MeCN)_5]O_2CCF_3$ may be due to a difficult reaction step such as the elimination of $O_2CCF_3^-$ from the co-ordination sphere [equation (2)].

$$cis\text{- or } trans\text{-}Ru(O_2CCF_3)_2(MeCN)_4 \xrightarrow{MeCN} [Ru(O_2CCF_3)(MeCN)_5]O_2CCF_3 \quad (2)$$

Table 5. Selected bond lengths (Å) and angles (°) for $Ru_2(\mu\text{-}O_2CCF_3)_4(thf)_2$*

O(1)–Ru(1)	2.070(6)	O(2)–Ru(1)	2.072(6)
O(3)–Ru(1)	2.076(6)	O(4)–Ru(1)	2.072(6)
O(5)–Ru(1)	2.268(6)	Ru(1)–Ru(1a)	2.276(3)
C(1)–O(1)	1.241(8)	C(3)–O(4)	1.243(8)
C(5)–O(5)	1.383(10)	C(8)–O(5)	1.403(10)
C(2)–C(1)	1.531(10)	F(1)–C(2)	1.251(10)
F(2)–C(2)	1.263(10)	F(3)–C(2)	1.289(9)
C(4)–C(3)	1.527(11)	F(4)–C(4)	1.248(10)
F(5)–C(4)	1.252(10)	F(6)–C(4)	1.286(9)
C(6)–C(5)	1.436(13)	C(7)–C(6)	1.418(15)
C(8)–C(7)	1.367(13)		
O(2)–Ru(1)–O(1)	178.8(2)	O(3)–Ru(1)–O(1)	92.2(3)
O(3)–Ru(1)–O(2)	87.5(3)	O(4)–Ru(1)–O(1)	87.8(3)
O(4)–Ru(1)–O(2)	92.5(3)	O(4)–Ru(1)–O(3)	179.1(2)
O(5)–Ru(1)–O(1)	91.1(3)	O(5)–Ru(1)–O(2)	90.1(3)
O(5)–Ru(1)–O(3)	89.5(3)	O(5)–Ru(1)–O(4)	91.4(3)
C(1)–O(1)–Ru(1)	116.1(5)	C(3)–O(4)–Ru(1)	115.9(5)
C(5)–O(5)–Ru(1)	125.6(6)	C(8)–O(5)–Ru(1)	124.7(6)
C(8)–O(5)–C(5)	107.5(7)	C(2)–C(1)–O(1)	115.9(7)
F(1)–C(2)–C(1)	114.6(7)	F(2)–C(2)–C(1)	109.5(7)
F(2)–C(2)–F(1)	108.9(9)	F(3)–C(2)–C(1)	112.3(7)
F(3)–C(2)–F(1)	106.8(8)	F(3)–C(2)–F(2)	104.3(8)
C(4)–C(3)–O(4)	115.8(7)	F(4)–C(4)–C(3)	114.3(8)
F(5)–C(4)–C(3)	110.4(8)	F(5)–C(4)–F(4)	108.3(9)
F(6)–C(4)–C(3)	113.9(7)	F(6)–C(4)–F(4)	104.0(9)
F(6)–C(4)–F(5)	105.3(9)	C(6)–C(5)–O(5)	108.1(9)
C(7)–C(6)–C(5)	105.5(9)	C(8)–C(7)–C(6)	108.2(9)
C(7)–C(8)–O(5)	109.3(9)		

* Key to symmetry operations relating designated atoms to reference atoms at (*x*, *y*, *z*): (a) $-x$, $-y$, $1.0 - z$.

Unlike the reaction[5] of other $Ru_2(\mu\text{-}O_2CR)_4$ species with MeCN or between $Ru_2(\mu\text{-}O_2CCF_3)_4$ and thf or Me_2CO, where weak 2:1 adducts, $Ru_2(\mu\text{-}O_2CR)_4L_2$, are formed, the reaction between $Ru_2(\mu\text{-}O_2CCF_3)_4$ and MeCN involves metal–metal bond cleavage to give monomers. The initial step may be the rapid formation of a 2:1 adduct, *i.e.* $Ru_2(\mu\text{-}O_2CCF_3)_4(MeCN)_2$, followed by a series of fast stepwise additions of MeCN ultimately leading to metal–metal bond cleavage and the formation of $Ru(O_2CCF_3)_2(MeCN)_4$ which then undergoes a slower reaction as in equation (2) and perhaps an even slower further reaction leading to the $[Ru(MeCN)_6]^{2+}$ ion.[15]

The sensitivity of $Ru_2(\mu\text{-}O_2CCF_3)_4$ to cleavage in MeCN, but not in thf or Me_2CO may be attributable to metal–NCMe π interaction which is significantly influenced by the nature of the R group of the bridging anion: thus, the species $Ru_2(\mu\text{-}O_2CR)_4$ (R = H, Me, Et, Ph, or CH_2Cl) form only 2:1 adducts.[5] Such an interaction has been postulated by Bear and co-workers[13] to account for the slightly higher reaction constant, ρ, for MeCN with respect to CH_2Cl_2, dimethylformamide (dmf), and Me_2SO in the electron-transfer reactions of dirhodium carboxylates. Girolami and Andersen[16] have previously shown the promotion of cleavage of M–M bonds generally by π-acceptor ligands and of the Ru_2^{5+} core of $[Ru_2(\mu\text{-}O_2CMe)_4Cl]_n$ by Bu^tNC specifically.

The structure of the trifluoroacetate–thf adduct $Ru_2(O_2CCF_3)_4(thf)_2$ is shown in Figure 2 and selected bond lengths and angles are given in Table 5. The structure is as expected, but differs from that of the analogous acetate–thf adduct[5] in two significant features. The Ru ··· Ru distance is longer [by *ca.* 0.015(3) Å] and the Ru–O(thf) distance shorter [by *ca.* 0.12(6) Å] in the trifluoroacetate, and this is consistent with the strong electron-withdrawing properties of the CF_3 group mentioned above.

(b) *Carbonato species.* Whereas structurally characterised

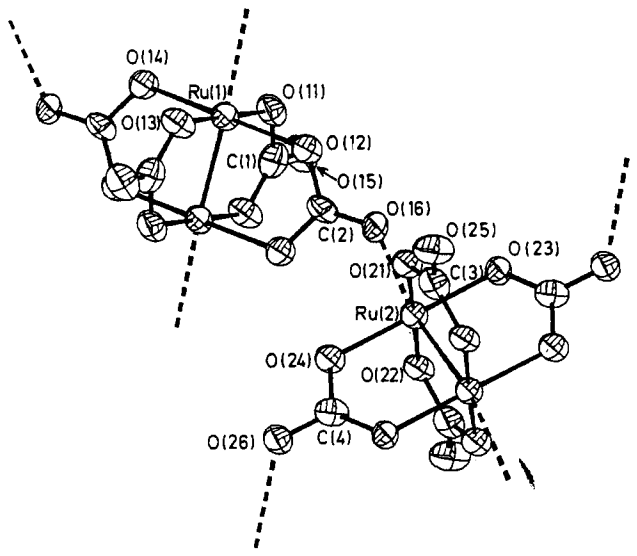

Figure 3. The structure of the polymeric anion in $\{Na_3[Ru_2(\mu\text{-}O_2CO)_4]\cdot 6H_2O\}_n$

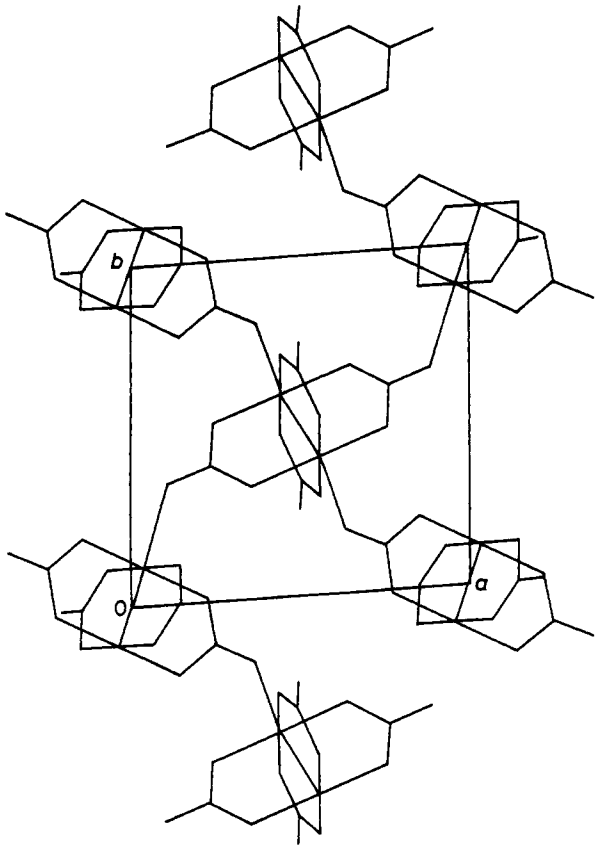

Figure 4. A projection of the unit-cell contents of $\{Na_3[Ru_2(\mu\text{-}O_2CO)_4]\cdot 6H_2O\}_n$ viewed down the *c* axis

carbonato anions $[M_2(\mu\text{-}O_2CO)_4(H_2O)_2]^{4-}$ (M = Cr[17,18] or Rh[19]) have long been known, carbonato species of ruthenium have remained elusive; the only compounds appear to be the impure (black) $Ru(CO)_2(PPh_3)_2(CO_3)$,[20] and the crystallographically characterised $Ru(bipy)_2(CO_3)$ (bipy = 2,2′-bipyridyl).[21]

The orange polymeric complex[22] $\{K_3[Ru_2(\mu\text{-}O_2CO)_4]\cdot 6H_2O\}_n$ is prepared in *ca.* 80% yield by heating an aqueous solution of $Ru_2(\mu\text{-}O_2CMe)_4$ under reflux with a two-fold excess of K_2CO_3. The reaction is disproportionative with the overall stoicheiometry approximating to that in equation (3).

$$5\,Ru_2(\mu\text{-}O_2CMe)_4 + 16\,K_2CO_3 \xrightarrow{H_2O} 2\,Ru^0 + 4\{K_3[Ru_2(\mu\text{-}O_2CO)_4]\cdot 6H_2O\}_n + 20\,K(O_2CMe) \quad (3)$$

The potassium salt is insoluble in organic solvents and poorly soluble in cold water, though more soluble in hot. The sodium salt, which is best made from the potassium salt by ion exchange is much more soluble in cold water.

Although the conductivities are slightly low[23] both the Na and K salts are best regarded as 3:1 electrolytes. Their i.r. spectra are virtually identical, having carbonate bands at 1 551, 1 490, 1 246, and 1 045 cm^{-1}. These bands differ substantially from those assigned to uni- or bi-dentate CO_3^{2-} [24] or bridging CO_3^{2-} in $Na_4[Rh_2(\mu\text{-}O_2CO)_4]\cdot 2.5H_2O$[19b] and suggest an unusual bonding mode. This has been confirmed by *X*-ray analysis (see below).

The electronic spectrum of the anion in H_2O ($\lambda_{max.}$ 413 nm, $\varepsilon_{max.}$ 873 $dm^3\ mol^{-1}\ cm^{-1}$) is similar to that of $Na_4[Rh_2(\mu\text{-}O_2CO)_4]\cdot 2.5H_2O$ though shifted to higher energy.[19b] In common with other complexes such as $[Ru_2(\mu\text{-}O_2CPr^n)_4Cl]_n$[1,7] or $[Ru_2(\mu\text{-}O_2CMe)_4X]_n$ (X = O_2CEt^- or $O_2CCF_3^-$), the Ru_2^{5+} core appears to have a $\sigma^2\pi^4\delta^2\pi^{*2}\delta^{*1}$ electronic configuration. This is supported by the magnetic susceptibility ($\mu_{eff.}$ = 2.9 B.M. per Ru at 295 K) which corresponds to three unpaired electrons per binuclear unit and a characteristic e.s.r. ($S = \frac{3}{2}$) spectrum ($g_\perp = g_\parallel = 2.1 \pm 0.1$), in H_2O–ethylene glycol glass at 77 K.

Cyclic voltammetric studies in 0.1 mol dm^{-3} $NaPF_6$ or NaCl–H_2O solutions at 293 K show that the anion undergoes a reversible one-electron oxidation at +0.59 V; no reduction is observed before the solvent front. The ability of the relatively 'hard' CO_3^{2-} ligand to stabilise the $Ru_2^{5+/6+}$ core is in sharp contrast to that of the relatively 'soft' O_2CR^- ligand which generally stabilises the $Ru_2^{4+/5+}$ [1,5,7] core, or even the $Ru_2^{3+/4+}$ core in the case of $O_2CCF_3^-$.

X-Ray analysis of the sodium salt shows that the structure is polymeric in the solid state. The crystal contains centrosymmetric $Ru_2(O_2CO)_4$ dimers which are linked into layers *via* axial O · · · Ru interactions involving free oxygen atoms of one centrosymmetric pair of carbonates as shown in Figures 3 and 4. The Ru–O distances to the bridging oxygens (Table 6) are slightly shorter than those in the dimers previously described,[5] consistent with the increase in average oxidation state of the metal atoms in the present structure. These, and the Ru–Ru distance, slightly shorter than for the Ru^{II}–Ru^{II} dimers, are similar to values found for other Ru^{II}–Ru^{III} structures.[1] The two independent axial O · · · Ru distances differ slightly (Table 6), but are of the same order as the bonds to the axial oxygen donors in the molecular species. The involvement of some of the carbonate oxygens in these interactions has only a marginal effect on the C–O bond length. The water molecules present in the structure are associated only with the sodium ions, whose co-ordination also involves strong interactions with carbonate oxygen atoms (Table 6).

The potassium salt reacts with a non-degassed CF_3CO_2H–$(CF_3CO)_2O$ mixture to yield an orange microcrystalline air-stable precipitate which is insoluble in non-co-ordinating solvents such as hexane, toluene, and CH_2Cl_2 and decomposes instantly in more co-ordinating solvents such as Et_2O, Me_2CO, thf, and MeCN. Analytical data (Table 1) indicate the complex is $Ru_2(O_2CCF_3)_5$ while mass spectral data, in the high-mass region, shows ($M^+ - O_2CCF_3$), *i.e.* $[Ru_2(O_2CCF_3)_4]^+$. This complex is also paramagnetic ($\mu_{eff.}$ = 2.9 B.M. per Ru at

Table 6. Selected bond lengths (Å) and angles (°) for $\{Na_3[Ru_2(\mu\text{-}O_2CO)_4]\cdot 6H_2O\}_n$

(*a*) In $[Ru_2(\mu\text{-}O_2CO)_4]_n$ system			
O(11)–Ru(1)	2.014(8)	O(12)–Ru(1)	2.021(7)
O(13)–Ru(1)	2.033(7)	O(14)–Ru(1)	2.022(7)
O(26)–Ru(1a)	2.310(7)	Ru(1)–Ru(1b)	2.255(3)
O(16)–Ru(2)	2.240(7)	O(21)–Ru(2)	2.016(7)
O(22)–Ru(2)	2.021(7)	O(23)–Ru(2)	2.025(7)
O(24)–Ru(2)	2.025(7)	Ru(2)–Ru(2c)	2.253(7)
C(1)–O(11)	1.336(11)	C(2)–O(12)	1.296(10)
C(1)–O(15)	1.246(10)	C(2)–O(16)	1.257(9)
C(3)–O(21)	1.318(10)	C(4)–O(24)	1.315(10)
C(3)–O(25)	1.239(10)	C(4)–O(26)	1.270(10)
O(12)–Ru(1)–O(11)	88.6(3)	O(13)–Ru(1)–O(11)	179.6(1)
O(13)–Ru(1)–O(12)	91.1(3)	O(14)–Ru(1)–O(11)	90.3(3)
O(14)–Ru(1)–O(12)	178.8(2)	O(14)–Ru(1)–O(13)	90.0(3)
O(26)–Ru(1)–O(11)	87.5(3)	O(26)–Ru(1)–O(12)	95.2(3)
O(26)–Ru(1)–O(13)	92.4(3)	O(26)–Ru(1)–O(14)	85.2(3)
O(21)–Ru(2)–O(16)	85.2(3)	O(22)–Ru(2)–O(16)	95.3(3)
O(22)–Ru(2)–O(21)	178.2(2)	O(23)–Ru(2)–O(16)	81.2(3)
O(23)–Ru(2)–O(21)	89.8(3)	O(23)–Ru(2)–O(22)	92.0(3)
O(24)–Ru(2)–O(16)	98.8(3)	O(24)–Ru(2)–O(21)	89.9(3)
O(24)–Ru(2)–O(22)	88.4(3)	O(24)–Ru(2)–O(23)	179.6(1)
C(1)–O(11)–Ru(1)	120.6(6)	C(2)–O(12)–Ru(1)	121.9(6)
C(2)–O(16)–Ru(2)	135.8(5)	C(3)–O(21)–Ru(2)	121.6(6)
C(4)–O(24)–Ru(2)	118.7(6)	C(4)–O(26)–Ru(1)	126.5(6)
O(15)–C(1)–O(11)	119.0(9)	O(16)–C(2)–O(12)	119.3(8)
O(25)–C(3)–O(21)	120.8(8)	O(26)–C(4)–O(24)	117.4(8)
(*b*) Na co-ordination			
O(12)–Na(1)	2.475(9)	O(01)–Na(1)	2.350(13)
O(03)–Na(1)	2.395(9)	O(25)–Na(2)	2.327(8)
O(01)–Na(2)	2.451(11)	O(04)–Na(3)	2.361(14)
O(06)–Na(3)	2.388(14)	O(14)–Na(4)	2.567(14)
O(04)–Na(4)	2.297(12)		
O(01)–Na(1)–O(03)	95.5(4)	O(12)–Na(1)–O(03)	83.8(3)
O(12)–Na(1)–O(01)	109.3(4)	O(25)–Na(2)–O(01)	89.8(3)
O(04)–Na(3)–O(04)	97.4(5)	O(14)–Na(4)–O(04)	101.0(5)

* Key to symmetry operations relating designated atoms to reference atoms at (*x*, *y*, *z*): (a) *x*, −1.0 + *y*, *z*; (b) −*x*, −*y*, −*z*; (c) 1.0 − *x*, −1.0 − *y*, −*z*.

295 K) consistent with three unpaired electrons per binuclear unit and may therefore possess the $\sigma^2\pi^4\delta^2\pi^{*2}\delta^{*1}$ electronic configuration of a metal–metal bonded Ru_2^{5+} core species. The i.r. spectrum shows strong $\nu_{asym}(CO_2)$ bands at 1 620 and 1 539 cm^{-1} and weaker $\nu_{sym}(CO_2)$ bands at 1 471 and 1 462 cm^{-1} attributable to bridging $O_2CCF_3^-$ ligands: the low frequency of $\nu_{asym}(CO_2)$ makes the presence of either ionic or unidentate $O_2CCF_3^-$ ligands highly unlikely.[8] The complex is best formulated as $[Ru_2(\mu\text{-}O_2CCF_3)_4(O_2CCF_3)]_n$, *i.e.* a new addition to the series $[Ru_2(\mu\text{-}O_2CR)_4X]_n$; as noted earlier, such compounds show small Δν values for the tetrabridge carboxylate and relatively large Δν values for the single carboxylato bridge (Table 2). This formulation also helps explain the decomposition in co-ordinating solvents, such as thf and acetone, since species of the type $[Ru_2(\mu\text{-}O_2CR)_4X]_n$ are readily solvated by co-ordinating solvents to give compounds[7,9] such as $[Ru_2(\mu\text{-}O_2CR)_4L_2]^+$, and as shown above electrochemically, the complexes $Ru_2(\mu\text{-}O_2CCF_3)_4L_2$ (L = Me_2CO or thf) are incapable of sustaining the II/III oxidation state.

Interaction of the carbonate with CF_3CO_2H–$(CF_3CO)_2O$ under H_2 (7 atm) in the presence of a weakly co-ordinating solvent such as Et_2O leads to $Ru_2(\mu\text{-}O_2CCF_3)_4(thf)_2$ upon recrystallisation from thf–n-hexane. This method which has previously been used to prepare $Cr_2(\mu\text{-}O_2CCF_3)_4(Et_2O)_2$[25] is an easier and more efficient way of making $Ru_2(\mu\text{-}O_2CCF_3)_4(thf)_2$ than that described earlier.

(c) *Triazenido species.* Triazenido complexes $M_2(\mu\text{-}N_3R_2)_4$ are known for M = Cu,[2] Cr,[26] Mo[26] and perhaps Rh,[27] but ruthenium complexes[28] are essentially confined to $RuCl(CO)(PPh_3)_2(N_3R_2)$, $Ru(PPh_3)_2(N_3R_2)_2$, $RuH(PPh_3)_3(N_3R_2)$, and $RuH(CO)(PPh_3)_2(N_3R_2)$ which have η^2-RN_3R and Ru^{II}.

Stirring a suspension of $Ru_2(\mu\text{-}O_2CMe)_4$ with four equivalents of $Li[N_3Ph_2]$ in Et_2O leads to an air-stable red-purple crystalline complex $Ru_2(\mu\text{-}N_3Ph_2)_4$; the mass spectrum shows the parent ion at *m/e* = 986.

Unlike other bridged Ru_2^{4+} core species noted earlier and the unbridged complexes Ru_2L_2 (L = a porphyrin[29] or tetraaza[14]annulene[1]) which are paramagnetic (two unpaired electrons per binuclear unit), $Ru_2(\mu\text{-}N_3Ph_2)_4$ is diamagnetic.

We have been unable to obtain crystals of *X*-ray quality so that we can only speculate on the structure, possibilities for which are shown diagrammatically (⌒ = PhN_3Ph) below.

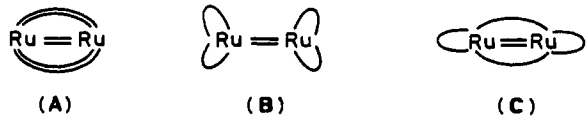

(A) (B) (C)

Structure (**C**) is disfavoured on the basis of variable-temperature ^1H n.m.r. spectra (Table 3), since only one type of phenyl resonance, characterised by α, β, and γ protons at δ 7.13 (d), 7.66 (t), and 6.56 (t) respectively, is observed. Although there have been attempts[30] to differentiate between unidentate, bidentate, and bridging triazenido groups on the basis of i.r. spectra, the number of disparities make it virtually impossible to be unequivocal. The general complexity of the 'characteristic' triazenido ligand i.r. region (1 100—1 600 cm^{-1}) in $Ru_2(\mu\text{-}N_3Ph_2)_4$, which shows bands at 1 593, 1 487, 1 456, 1 330, 1 309, 1 290, 1 264, 1 210, 1 170, and 1 158 cm^{-1}, strongly suggests the ligands are not exclusively chelating and therefore disfavours structure (**B**). The complex is best described by (**A**) on the basis of spectroscopic data as well as by analogy with related complexes of other metals[26] and in its ability to form stable axial adducts as noted below.

The unique diamagnetism of the complex suggests a $\sigma^2\pi^4\delta^2\pi^{*4}$ electronic configuration, which is presumably due to mixing of metal–metal orbitals and metal–ligand orbitals. As in the case of $Rh_2(\mu\text{-}O_2CR)_4$ and $Rh_2(\mu\text{-}mhp)_4\cdot CH_2Cl_2$ this mixing perturbs the normal $\delta^* < \pi^*$ ordering, which is predicted by metal–metal bonding considerations alone.[1]

Two other distinctly different δ^*, π^* orbital ordering cases have been previously noted in multiply metal–metal bonded Ru_2^{4+} core compounds. In the unbridged Ru_2L_2 complexes, noted above, the molecular orbitals of the ligands, L, appear to interact more weakly, or in a different way, with the metal–metal orbitals giving the normal $\delta^* < \pi^*$ ordering and leading to a $\sigma^2\pi^4\delta^2\delta^{*2}\pi^{*2}$ electronic configuration and two unpaired electrons per binuclear unit. The other case involves the bridged complexes $Ru_2(\mu\text{-}O_2CR)_4$[5] and $Ru_2(\mu\text{-}mhp)_4\cdot CH_2Cl_2$,[12] where the degree of metal–metal and metal–ligand mixing is presumed to be intermediate between the first two cases such that the δ^* orbital is only slightly higher/lower in energy than the π^* orbital and the virtually degenerate metal–metal π^* orbitals and δ^* orbital are singly occupied, leading to a $\sigma^2\pi^4\delta^2\pi^{*3}\delta^{*1}$ or $\sigma^2\pi^4\delta^2\delta^{*1}\pi^{*3}$ electronic configuration and two unpaired electrons per binuclear unit.

Cyclic voltammetric studies on $Ru_2(\mu\text{-}N_3Ph_2)_4$ in CH_2Cl_2 (Figure 5, Table 7) show some complexity. Comparing the redox potentials with those of its adducts (see below) it is evident that the potential of the most difficult oxidation is almost invariant at *ca.* +1.32 V. This oxidation we consider to be essentially

Table 7. Cyclic voltammetry of $Ru_2(\mu\text{-}N_3Ph_2)_4$ and its derivatives in 0.2 mol dm^{-3} $NBu^n{}_4PF_6$–CH_2Cl_2

	$E_{\frac{1}{2}}/V$[a]			
Complex	$Ru^I{}_2$–Ru^IRu^{II}	Ru^IRu^{II}–$Ru^{II}{}_2$	$Ru^{II}{}_2$–$Ru^{II}Ru^{III}$	
$Ru_2(\mu\text{-}N_3Ph_2)_4$	—	*−1.06*	*+0.16*	*+1.28*[b]
$Ru_2(\mu\text{-}N_3Ph_2)_4(NO)_2$[c]	[−1.75]	*−0.95*	*+0.54*	*+1.33*[b]
$Ru_2(\mu\text{-}N_3Ph_2)_4(Bu^tNC)$	—	*−1.05*	*+0.23*	*+1.36*[b]
$Ru_2(\mu\text{-}N_3Ph_2)_4(CO)_2$	*−1.76*	*−0.72*	(+0.59)	*+1.32*[b]

[a] As under Table 4. [b] These redox couples are believed to represent processes which are essentially ligand based. [c] Formally the redox couples are no longer $Ru^I{}_2$–Ru^IRu^{II}, Ru^IRu^{II}–$Ru^{II}{}_2$, and $Ru^{II}{}_2$–$Ru^{II}Ru^{III}$ but $Ru^0{}_2$–Ru^0Ru^I, Ru^0Ru^I–$Ru^I{}_2$, and $Ru^I{}_2$–Ru^IRu^{II} respectively.

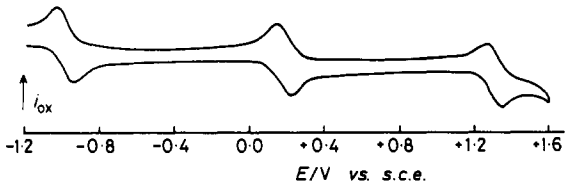

Figure 5. Cyclic voltammogram for $Ru_2(\mu\text{-}N_3Ph_2)_4$ in 0.2 mol dm^{-3} $NBu^n{}_4PF_6$–CH_2Cl_2; potential sweep rate 100 mV s^{-1}

ligand based. The potentials of the easier oxidation and the reduction of adducts of $Ru_2(\mu\text{-}N_3Ph_2)_4$ vary considerably which suggests that these are predominantly metal-based processes connecting the I/II–II/II and II/II–II/III oxidation states. The $N_3Ph_2^-$ ligand is thus stabilising the $Ru_2{}^{3+/4+/5+}$ core.

Unlike the carboxylates, the triazenido compound shows no tendency to form adducts with weak donor ligands such as thf, Me_2CO, or MeCN though it does form adducts with NO, Bu^tNC, and CO.

Axial Adducts of $Ru_2(\mu\text{-}O_2CR)_4$ *and* $Ru_2(\mu\text{-}N_3Ph_2)_4$.—The formation of weak complexes $Ru_2(\mu\text{-}O_2CR)_4L_2$ (L = H_2O, thf, Me_2CO, MeCN, or MeOH)[5] is characteristic of other transition-metal carboxylates $M_2(\mu\text{-}O_2CR)_4L_2$ (M = Cr, Mo, W, or Rh).[1,31] These $M_2{}^{4+}$ core species may also form adducts with stronger N, P, and C π-bonding ligands.[1,16,31] Adducts of $M_2(\mu\text{-}N_3R_2)_4$ (M = Cr or Mo)[26] are unknown and as noted above the ruthenium compound does not give adducts with thf, Me_2CO, or MeCN.

Nitrogen monoxide. The paramagnetic complexes $Ru_2(\mu\text{-}O_2CR)_4$ (R = Me, Et, Ph, or CF_3) (two unpaired electrons per binuclear unit) react readily in thf or Et_2O with nitrogen monoxide to yield red-orange microcrystalline precipitates (R = Me or Ph) or deep red solutions (R = Et or CF_3), from which red air-stable diamagnetic crystals of the bis-NO adducts may be isolated (Table 1).

The i.r. spectra (Table 2) have $\nu_{asym}(CO_2)$ and $\nu_{sym}(CO_2)$ bands at values close to those in their parent compounds. The propionate also shows two very strong broad ν(NO) bands at 1 722 and 1 748 cm^{-1} in the mull which collapse to a single narrow band at 1 745 cm^{-1} in hexane solution. The trifluoroacetate shows only a single broad ν(NO) at 1 800 cm^{-1} in the solid and a single narrow band at 1 805 cm^{-1} in hexane.

The relatively high value of the ν(NO) band for the trifluoroacetate compared to the propionate is attributable to the reduced M $d\pi \longrightarrow \pi^*(NO)$ backbonding which is probably due to the electron-withdrawing nature of the CF_3 group, which lowers the electron density on the metal centre. Despite the fact that both ν(NO) values are rather low for linear metal nitrosyls, this still appears to be a better interpretation than that of bent

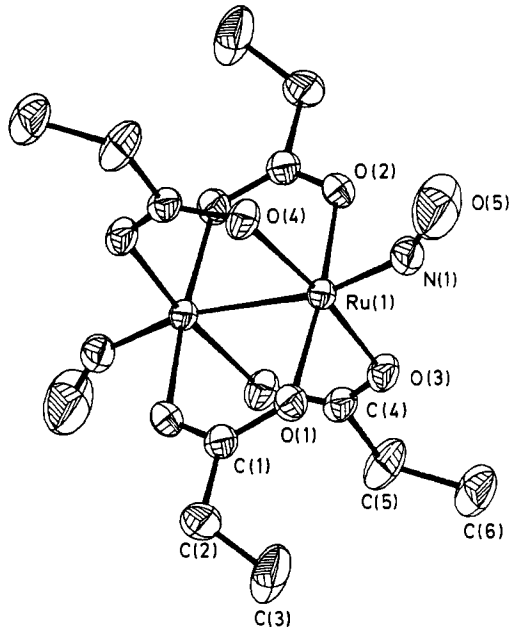

Figure 6. The structure of $Ru_2(\mu\text{-}O_2CEt)_4(NO)_2$

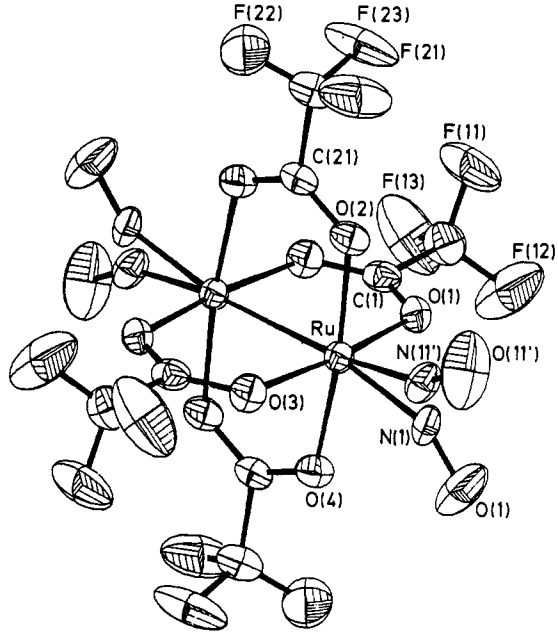

Figure 7. The structure of $Ru_2(\mu\text{-}O_2CCF_3)_4(NO)_2$

or bridging nitrosyls which would have ν(NO) bands at still lower values.[2] Linearity of the M–N–O group is also in accord with the empirical rules of Haymore and Ibers.[32] The identity of the complexes has been confirmed by *X*-ray crystallography as bis(nitrosyl) axial adducts of $Ru_2(\mu\text{-}O_2CR)_4$ (R = Et or CF_3), but in both cases, the Ru–N–O grouping is substantially bent, with angles of *ca.* 153(2)°. Diagrams of the two structures are shown in Figures 6 and 7, whilst selected bond lengths and angles are given in Table 8. In both complexes there is also a small bend of the Ru–N bond away from the line of the Ru–Ru axis, in the same direction as the bending at N, and in the case of the trifluoroacetate complex, the nitrosyls show two-fold disordering with (53:47 occupancies). The Ru–Ru distances in both NO compounds are *ca.* 0.25 Å longer than in the simple donor complexes, which is consistent with a formal reduction in

Table 8. Selected bond lengths (Å) and angles (°) for $Ru_2(\mu\text{-}O_2CR)_4(NO)_2$ (R = Et or CF_3)*

R = Et			
O(1)–Ru(1)	2.047(6)	O(2)–Ru(1)	2.056(6)
O(3)–Ru(1)	2.041(5)	O(4)–Ru(1)	2.065(5)
N(1)–Ru(1)	1.781(7)	Ru(1)–Ru(1a)	2.515(4)
C(1)–O(1)	1.262(7)	C(4)–O(3)	1.255(7)
O(5)–N(1)	1.126(8)	C(2)–C(1)	1.507(10)
C(3)–C(2)	1.362(11)	C(5)–C(4)	1.501(10)
C(6)–C(5)	1.448(11)		
O(2)–Ru(1)–O(1)	171.9(1)	O(3)–Ru(1)–O(1)	88.1(2)
O(3)–Ru(1)–O(2)	90.2(3)	O(4)–Ru(1)–O(1)	90.7(3)
O(4)–Ru(1)–O(2)	89.9(3)	O(4)–Ru(1)–O(3)	171.9(1)
N(1)–Ru(1)–O(1)	98.6(3)	N(1)–Ru(1)–O(2)	89.5(3)
N(1)–Ru(1)–O(3)	103.3(3)	N(1)–Ru(1)–O(4)	84.8(3)
C(1)–O(1)–Ru(1)	119.6(4)	C(4)–O(3)–Ru(1)	118.5(4)
O(5)–N(1)–Ru(1)	152.4(5)	C(2)–C(1)–O(1)	117.5(6)
C(3)–C(2)–C(1)	116.4(7)	C(5)–C(4)–O(3)	118.5(6)
C(6)–C(5)–C(4)	117.5(7)		
R = CF_3			
O(1)–Ru(1)	2.060(7)	O(2)–Ru(1)	2.062(7)
O(3)–Ru(1)	2.053(7)	O(4)–Ru(1)	2.060(7)
N(1)–Ru(1)	1.844(21)	N(1′)–Ru(1)	1.786(19)
Ru(1)–Ru(1b)	2.532(4)	C(11)–O(1)	1.247(11)
C(21)–O(2)	1.244(10)	O(11)–N(1)	1.104(22)
O(11′)–N(1′)	1.121(24)	C(12)–C(11)	1.515(14)
F(11)–C(12)	1.271(13)	F(12)–C(12)	1.246(13)
F(13)–C(12)	1.291(14)	C(22)–C(21)	1.548(14)
F(21)–C(22)	1.288(13)	F(22)–C(22)	1.230(13)
F(23)–C(22)	1.283(12)		
O(2)–Ru(1)–O(1)	88.8(3)	O(3)–Ru(1)–O(1)	171.7(2)
O(3)–Ru(1)–O(2)	90.7(3)	O(4)–Ru(1)–O(1)	90.4(3)
O(4)–Ru(1)–O(2)	172.0(2)	O(4)–Ru(1)–O(3)	89.0(3)
N(1)–Ru(1)–O(1)	91.7(7)	N(1)–Ru(1)–O(2)	108.1(8)
N(1)–Ru(1)–O(3)	96.3(7)	N(1)–Ru(1)–O(4)	79.9(8)
N(1′)–Ru(1)–O(1)	97.9(7)	N(1′)–Ru(1)–O(2)	83.0(8)
N(1′)–Ru(1)–O(3)	90.2(7)	N(1′)–Ru(1)–O(4)	105.0(8)
C(11)–O(1)–Ru(1)	119.7(6)	C(21)–O(2)–Ru(1)	119.0(6)
O(11)–N(1)–Ru(1)	152.8(21)	O(11′)–N(1′)–Ru(1)	152.2(21)
C(12)–C(11)–O(1)	115.2(9)	F(11)–C(12)–C(11)	112.2(10)
F(12)–C(12)–C(11)	114.3(10)	F(12)–C(12)–F(11)	107.9(12)
F(13)–C(12)–C(11)	112.0(11)	F(13)–C(12)–F(11)	102.9(11)
F(13)–C(12)–F(12)	106.7(12)	C(22)–C(21)–O(2)	116.4(9)
F(21)–C(22)–C(21)	111.5(9)	F(22)–C(22)–C(21)	113.5(10)
F(22)–C(22)–F(21)	108.5(12)	F(23)–C(22)–C(21)	109.1(9)
F(23)–C(22)–F(21)	104.0(11)	F(23)–C(22)–F(22)	109.8(11)

* Key to symmetry operations relating designated atoms to reference atoms at (x, y, z): (a) 1.0 − x, 1.0 − y, −z; (b) 0.5 − x, 0.5 − y, 1.0 − z.

the oxidation state of the metal and lowering of the Ru–Ru bond order.

The bend at nitrogen in these formally Ru^I_2, $\{RuNO\}$,[7] complexes is not unexpected[33,34] since other six-co-ordinate $\{MNO\}^7$ species such as $[Fe\{C_6H_4(AsMe_2)_2\text{-}o\}_2(NO)Cl]^{2+}$ [Fe–N–O 148(2)°[33]] and $Ru_4(NO)_4(\mu\text{-}Cl)_4(\mu\text{-}PPh_2)_4$ [Ru–N–O 160.3(8)°[35]] show a similar behaviour. Partially bent M–N–O groups in six-co-ordinate $\{MNO\}^7$ compounds can be rationalised on the basis of linear-bent one-electron molecular orbital correlation diagrams.[33] The major effect of bending the MNO moiety in $\{MNO\}^7$ complexes is to modify the relative energies of the metal *d* orbitals and the NO π* orbitals in such a way as to lower the total energy of the complex.

The compounds $Ru_2(\mu\text{-}O_2CR)_4(NO)_2$ (R = Me, Et, Ph, or CF_3) are diamagnetic in the solid while for R = Et and CF_3 there are sharp solution n.m.r. spectra (Table 3). The ^1H n.m.r. spectrum of the propionate consists of a triplet at δ 1.06 ascribed to CH_3 protons and a quartet at δ 2.42 ($^3J_{HH}$ 7.6 Hz) ascribed to the CH_2 protons. The ^{19}F n.m.r. spectrum of the trifluoroacetate shows a singlet at δ −74.5 for the four equivalent CF_3 groups; ^{19}F n.m.r. spectra are said[36] to exhibit resonances at *ca.* δ −70[37] for bidentate and bridging $CF_3CO_2^-$ groups and at *ca.* δ −74[38] for unidentate or ionic groups. The similarity of solid and solution i.r. spectra indicates that the bridging structure is retained in solution and suggests, as has been previously noted,[8] that ^{19}F n.m.r. data are of limited utility in determining the mode of $CF_3CO_2^-$ bonding.

The metal–metal bonding scheme of Norman *et al.*[11] applied to the NO complexes would give $\sigma^2\pi^4\delta^2\pi^{*4}\delta^{*2}$ or $\sigma^2\pi^4\delta^2\delta^{*2}\pi^{*4}$ electronic configurations, accounting for the diamagnetism and the lengthening of the Ru–Ru distance to that compatible with a Ru–Ru single bond due to the addition of two extra electrons into antibonding orbitals. However, due to the similarity of the energies of the metal *d* orbitals and the π* orbitals of NO and the inadequacy of the formalistic argument, the real situation must be more complex.

Cyclic voltammetric studies on 0.2 mol dm^{-3} $NBu^n_4PF_6$–CH_2Cl_2 solutions of $Ru_2(\mu\text{-}O_2CEt)_4(NO)_2$ show a single reversible one-electron oxidation, formally Ru^I_2–Ru^IRu^{II} at +1.15 V and an irreversible reduction at −0.86 V. The shift of *ca.* 1.2 V to more positive potentials for the oxidation of $Ru_2(\mu\text{-}O_2CEt)_4(NO)_2$ with respect to $Ru_2(\mu\text{-}O_2CEt)_4L_2$ (L = thf or MeCN) is at least partially attributable to the ability of the NO ligand to accept delocalised π-electron density into its π* orbital. This effect in conjunction with the electron-withdrawing capability of the CF_3 groups leads to the non-observance of any oxidative process, or indeed any redox process within the solvent front, for $Ru_2(\mu\text{-}O_2CCF_3)_4(NO)_2$.

The deep purple $Ru_2(\mu\text{-}N_3Ph_2)_4$ in CH_2Cl_2 reacts rapidly with NO leading to the orange, diamagnetic $Ru_2(\mu\text{-}N_3Ph_2)_4(NO)_2$. The ^1H n.m.r. spectrum (Table 3) has a single sharp phenyl resonance at δ 7.13. The i.r. spectrum is similar to that of the precursor in the 1 100—1 600 cm^{-1} region but has an additional strong NO band at 1 757 cm^{-1} (1 755 cm^{-1} in toluene solution). The low value of this band [*cf.* $Ru_2(\mu\text{-}O_2CR)_4(NO)_2$ above] suggests a 'linear' rather than bent NO.

Unlike the carboxylate adducts which show parent ions in their mass spectra, $Ru_2(\mu\text{-}N_3Ph_2)_4(NO)_2$ shows only the parent ion of $Ru_2(\mu\text{-}N_3Ph_2)_4$. This is unsurprising since heating $Ru_2(\mu\text{-}N_3Ph_2)_4(NO)_2$ at *ca.* 140 °C under vacuum leads to formation of $Ru_2(\mu\text{-}N_3Ph_2)_4$. Heating $Ru_2(\mu\text{-}O_2CR)_4(NO)_2$ at higher temperature under vacuum leads to decomposition to several unidentified nitrosyl species.

Cyclic voltammetric studies on $Ru_2(\mu\text{-}N_3Ph_2)_4(NO)_2$ (Table 7) shows an even more complex electrochemistry than that of its parent. In addition to the three reversible redox processes noted earlier for $Ru_2(\mu\text{-}N_3Ph_2)_4$, the nitrosyl shows an irreversible second reduction at −1.75 V. Two of the three reversible redox couples move to more positive potentials as might be anticipated given the previously noted π-acceptor ability of the NO ligand. The other reversible redox process at *ca.* +1.33 V which is believed to be essentially ligand based, is only slightly perturbed *ca.* 50 mV from that in its parent compound. The shift of *ca.* 0.4 V to more positive potentials of the Ru^{II}_2–$Ru^{II}Ru^{III}$ redox couple upon co-ordination of two NO ligands is small in comparison to the *ca.* 1.2 V noted for the same redox couple upon NO ligand co-ordination of $Ru_2(\mu\text{-}O_2CEt)_4$. However, the latter shift is anomalously large since a range of only *ca.* 0.7 V is covered by the potentials observed for $Rh_2(\mu\text{-}O_2CEt)_4$ with various O, N, S, and P axial donors.[39]

Obviously there must be a very strong (σ + π) interaction between the paramagnetic $Ru_2(\mu\text{-}O_2CR)_4$ core (two unpaired electrons) and NO which will be aided by the similarity of the energies of the metal *d* orbitals and the π* orbitals of NO. Such

an axial interaction seems certain to cause significant modification of the molecular orbital diagram[11] for $Ru_2(\mu\text{-}O_2CH)_4$. This is necessary to account for the strength of the Ru–N bonds, the relative weakness of the Ru–O bonds, the diamagnetism and metal–metal bond multiplicity of $Ru_2(\mu\text{-}O_2CR)_4(NO)_2$, and the substantial lowering of the energy of the highest occupied molecular orbital (h.o.m.o.) for this compound as measured by the large increase in the $Ru^{II}{}_2$–$Ru^{II}Ru^{III}$ redox couple upon NO ligation.

The $(\sigma + \pi)$ interaction between the diamagnetic $Ru_2(\mu\text{-}N_3Ph_2)_4$ and NO is evidently much weaker and doubtless arises from a greater degree of orbital energy and symmetry mismatch than that operating in the carboxylate compounds. The weaker interaction is shown by the relative strength of the Ru–N(N) bonds in comparison to those of the Ru–N(O) bonds as demonstrated by the ready loss of NO on heating $Ru_2(\mu\text{-}N_3Ph_2)_4(NO)_2$ and the relatively small lowering of the energy of the h.o.m.o. as indicated electrochemically.

t-Butyl isocyanide. The complexes $Ru_2(\mu\text{-}O_2CR)_4(thf)_2$ (R = Me or CF_3) react with excess Bu^tNC in MeOH–Et_2O (1:1) and hexane respectively to yield the white, metal–metal bond cleaved products, $Ru(O_2CR)_2(Bu^tNC)_4$. The acetate, *trans*-$Ru(O_2CMe)_2(Bu^tNC)_4$, has been made previously by interaction of $[Ru_2(\mu\text{-}O_2CMe)_4Cl]_n$ and excess Bu^tNC and shown to have the *trans* configuration with unidentate acetates.[16]

The i.r. spectrum of $Ru(O_2CCF_3)_2(Bu^tNC)_4$ (Table 2) shows a strong $\nu(CO_2)_{asym}$ band at 1 715 cm^{-1} and a weak $\nu_{sym}(CO_2)$ band at *ca.* 1 405 cm^{-1} with $\Delta\nu$ *ca.* 300 cm^{-1} consistent with unidentate $CF_3CO_2^-$.[8] The ν(CN) region shows two strong bands at 2 175 and 2 150 cm^{-1} and two weaker bands at 2 225 and 2 080 cm^{-1} (corresponding strong and weak bands occur in CH_2Cl_2 solution at 2 176 and 2 145 cm^{-1} and 2 222 and 2 070 cm^{-1} respectively) consistent with the formulation *cis*-$Ru(O_2CCF_3)_2(Bu^tNC)_4$. The ^1H n.m.r. spectrum (Table 3) shows two slightly broadened singlets (δ 1.14 and 1.05) for the *cis* isomer.

Different isomers of $Ru(O_2CR)_2(Bu^tNC)_4$ for R = Me and CF_3 may be due to the differing reaction conditions employed, or to steric and electronic considerations. Both *cis*- and *trans*-isomers are known for related species such as $RuCl_2(EtNC)_4$.[40]

The reaction of $Ru_2(\mu\text{-}N_3Ph_2)_4$ with excess Bu^tNC in toluene at ambient temperature leads to the diamagnetic $Ru_2(\mu\text{-}N_3Ph_2)_4(Bu^tNC)$. The ^1H n.m.r. spectrum (Table 3) is consistent with a 1:1 adduct. The phenyl region consists of a complex multiplet between δ 6.5—7.5 and the CH_3 region of a sharp singlet at δ 1.03. The i.r. spectrum is similar to that of the precursor in the 1 100—1 600 cm^{-1} region but has an additional strong ν(CN) band at 2 120 cm^{-1} (2 117 cm^{-1} in toluene).

Like the bis(nitrosyl) this isocyanide readily loses the axial ligand upon heating; the mass spectrum is that of the precursor.

Cyclic voltammetric studies (Table 7) shows behaviour more similar to that of $Ru_2(\mu\text{-}N_3Ph_2)_4$ than that of the dinitrosyl and dicarbonyl compounds (below). Whereas for the latter, metal-based redox couples shift by up to 0.4 V to more positive potentials with respect to the parent, the same couples are shifted by <0.1 V for $Ru_2(\mu\text{-}N_3Ph_2)_4(Bu^tNC)$. These differences can be rationalised in two ways. First, the good σ-donor ability of Bu^tNC helps off-set the shift to more positive potentials caused by its strong π-acceptor ability; by comparison, both NO and CO are poor σ donors but still good π acceptors. Secondly, for Bu^tNC only one axial ligand is bound to the Ru_2^{4+} core, whereas for the NO and CO complexes, there are two.

The reason why $Ru_2(\mu\text{-}N_3Ph_2)_4$ co-ordinates only one isocyanide must be steric. Despite the compactness of Bu^tNC (cone angle 70°[41]) and its essential linearity, it is still large compared to NO or CO. Severe twisting of some or all the phenyl groups of the bridging ligands must occur in order to accommodate Bu^tNC. This distortion may then block the other axial site.

There are numerous examples of metal–metal multiple bond cleavage by both alkyl and aryl isocyanides;[42] even under mild conditions Bu^tNC cleaves the metal–metal multiple bonds in $Mo_2(\mu\text{-}O_2CR)_4$, $Re_2(\mu\text{-}O_2CR)_4Cl_2$, and $[Ru_2(\mu\text{-}O_2CR)_4Cl]_n$, though not the metal–metal single bond of $Rh_2(\mu\text{-}O_2CR)_4$ which forms $Rh_2(\mu\text{-}O_2CR)_4(Bu^tNC)_2$.[16] That a complex with a single metal–metal bond remains intact while complexes with higher M–M bond orders cleave to give mononuclear products can be readily explained. As shown for $Rh_2(\mu\text{-}O_2CR)_4$,[43] co-ordination by good π-acceptor ligands strengthens the Rh–Rh single bond by effectively delocalising electron density from the metal–metal antibonding h.o.m.o.s. Conversely, for molybdenum and rhenium the h.o.m.o.s are metal–metal bonding and co-ordination by π-acceptors leads to bond weakening. However, for $[Ru_2(\mu\text{-}O_2CR)_4Cl]_n$ co-ordination by Bu^tNC apparently leads to delocalisation of electron density, not only from the antibonding h.o.m.o.s, but also from the M–M bonding orbitals of proper symmetry which lie just slightly lower in energy, which causes net weakening of the bond.[11]

It seems likely that a similar delocalisation of electron density from both bonding and antibonding orbitals occurs in the case of $Ru_2(\mu\text{-}O_2CR)_4$ (R = Me or CF_3), thus leading to the formation of monomeric complexes on reaction with Bu^tNC. The complex $Ru_2(\mu\text{-}N_3Ph_2)_4$, which may have the diamagnetic electronic configuration $\sigma^2\pi^4\delta^2\pi^{*4}$ [*cf.* the paramagnetic electronic configuration of $\sigma^2\pi^4\delta^2\pi^{*3}\delta^{*1}$ for $Ru_2(\mu\text{-}O_2CR)_4$], behaves towards Bu^tNC in a similar way to $Rh_2(\mu\text{-}O_2CMe)_4$. This suggests that electron density is delocalised essentially from the metal–metal antibonding h.o.m.o.s with little or no involvement from M–M bonding orbitals of proper symmetry, which must, in contrast to the situation for $Ru_2(\mu\text{-}O_2CR)_4^{0/+}$, be of considerably lower energy.

Carbon monoxide. The complexes $Ru_2(\mu\text{-}O_2CR)_4(thf)_2$ (R = CF_3 or Me) are readily cleaved by CO (ambient temperature, *ca.* 3.5 atm CO). The trifluoroacetate gives *fac*-$Ru(O_2CCF_3)_2(CO)_3(thf)$ (Table 1) but the acetate gives a mixture of products that we have not studied further.

The mass spectrum of the trifluoroacetate has no parent ion but shows ions for $[Ru(O_2CCF_3)_2(CO)_3]^+$ and $[thf]^+$ at *m/e* 411 and 72 respectively. The i.r. spectrum (Table 2) shows a strong $\nu_{asym}(CO_2)$ at 1 700 cm^{-1} and a weak $\nu_{sym}(CO_2)$ at 1 410 cm^{-1} ($\Delta\nu$ = 290 cm^{-1}) which is consistent with unidentate co-ordination. The three CO stretches ($2A' + A''$) are consistent with the C_s symmetry of the octahedral *fac* isomer.

Although numerous complexes, *fac*-$RuX_2(CO)_3(thf)$, are known[44] for X = Cl^-, Br^-, and I^-, none is known for X = $O_2CCF_3^-$. The thf is relatively strongly bound in *fac*-$Ru(O_2CCF_3)_2(CO)_3(thf)$ whereas in *fac*-$RuCl_2(CO)_3(thf)$ spontaneous dissociation forms $Ru_2Cl_4(CO)_6$.[45] The stronger co-ordination of thf in the trifluoroacetate is probably a reflection of the electron-withdrawing ability of the $O_2CCF_3^-$ ligand compared with Cl^-.

Interaction of $Ru_2(\mu\text{-}N_3Ph_2)_4$ and CO (2 atm) in toluene leads to the purple-blue microcrystalline $Ru_2(\mu\text{-}N_3Ph_2)_4(CO)_2$, which readily gives $Ru_2(\mu\text{-}N_3Ph_2)_4$ on heating. Cyclic voltammetry shows similarities with the nitrosyl, the potentials reflecting the roughly comparable σ-donor/π-acceptor properties of CO and NO although CO preferentially stabilises the lower oxidation states.

Metal–metal multiple bond fission by CO[42] is less common than that for isocyanides and the reaction conditions required are generally more vigorous, *e.g.* $Mo_2(\mu\text{-}O_2CCF_3)_4$ does not react with CO (18 atm) but is readily cleaved by Bu^tNC to give $[Mo(O_2CCF_3)(Bu^tNC)_6]O_2CCF_3$.[16] This was rationalised on the basis of the greater σ-donor ability of isocyanide. Although

the complexes $Mo_2(\mu\text{-}O_2CR)_4$ do not readily react or form adducts, with weak σ-donor ligands such as Me_2CO, thf, or MeOH, their ruthenium analogues do and presumably it is this intrinsic ability of the $Ru^{II}{}_2$ complexes that allows initial co-ordination of CO.

Triphenylphosphine. The carboxylates react with two equivalents of PPh_3 in methanol to yield the known[46] orange $Ru(O_2CR)_2(PPh_3)_2$ (R = Me or CF_3). The previously unreported variable-temperature ^1H and ^{19}F n.m.r. spectra of $Ru(O_2CCF_3)_2(PPh_3)_2$ are given in Table 3.

Metal–metal bond cleavage of $Rh_2(\mu\text{-}O_2CCF_3)_4$[47] by PPh_3 under mild conditions gives Rh^I and Rh^{III} monomers. Ligand-induced polarization of the Rh–Rh bond, and not disproportionation of unstable Rh^{II} monomers formed upon homolytic cleavage of the Rh–Rh bond, was proposed. In the present Ru case where only monomeric Ru^{II} species are formed, homolytic Ru–Ru bond cleavage probably occurs. The failure of PPh_3 to cleave the triazenido complex is presumably due to steric factors inhibiting co-ordination of PPh_3.

Acetonitrile. Unlike the reaction of $Ru_2(\mu\text{-}O_2CR)_4$ (R = H, Me, Et, Ph, or CH_2Cl) with MeCN which leads to formation of weak bis adducts,[5] the trifluoroacetate is cleaved by MeCN as noted earlier. The final product of the ambient temperature reaction is the white microcrystalline salt, $[Ru(O_2CCF_3)(MeCN)_5]O_2CCF_3$, which is a 1:1 electrolyte in MeCN. The i.r. spectrum (Table 2) indicates both ionic and unidentate trifluoroacetate environments.

The ^1H n.m.r. spectrum (Table 3) consists of two singlets for the methyl resonances in a ratio of 1:4 at δ 2.31 and 2.49 respectively; the ^{19}F n.m.r. spectrum has two singlets of equal intensity at δ −72.7 and −72.6 for ionic and unidentate trifluoroacetate environments.

No reaction occurs between $Ru_2(\mu\text{-}N_3Ph_2)_4$ and MeCN; possibly because MeCN is not a sufficiently good σ donor or π acceptor to allow co-ordination.

Pyridine. The complexes $Ru_2(\mu\text{-}O_2CR)_4$ (R = Me or CF_3) react with excess pyridine (py) in methanol and Et_2O respectively to yield the Ru–Ru bond cleaved products $Ru(O_2CR)_2(py)_4$; the acetate is known[6] from interaction of pyridine and $[Ru_2(\mu\text{-}O_2CMe)_4Cl]_n$. Spectroscopic data (Tables 2 and 3) are consistent with *trans*-unidentate carboxylate.

In summary therefore the complexes $Ru_2(\mu\text{-}O_2CR)_4$ (R = Me or CF_3) are cleaved both by π-acceptor ligands such as RNC, CO, and PR_3 and also by ligands such as pyridine which are normally regarded as strong σ-donors with poor π-acceptor ability. The cleavage of multiple bonds by strong σ-donor ligands is a well recognised, if poorly understood, phenomenon.[42]

The failure of pyridine to react with $Ru_2(\mu\text{-}N_3Ph_2)_4$ may be due, as for PPh_3, to steric constraints imposed by the bulky phenyl groups of the triazenido ligands.

Conclusions

The reactivity of the paramagnetic complexes $Ru_2(\mu\text{-}O_2CR)_4$ (R = Me or CF_3) towards Lewis bases is remarkably similar and unlike that of the diamagnetic molybdenum and rhodium analogues. Both Ru compounds form axial (class I) 2:1 adducts with weak σ-donor ligands, with little or no π-acceptor ability, such as thf.[5] Both are readily cleaved to give monomeric compounds with strong π-acceptor ligands such as Bu^tNC or CO or weaker π-acceptor ligands such as PPh_3 or pyridine; both form strong class I, 2:1 complexes with NO. The only major disparity arises for the weak σ-donor, π-acceptor MeCN. The acetate forms a class I 2:1 adduct while the trifluoroacetate undergoes Ru–Ru bond fission to give monomers. The cleavage of $Ru_2(\mu\text{-}O_2CCF_3)_4$ by MeCN is probably a consequence of metal–metal bond weakening through Ru(dπ)–π*(MeCN) back-bonding of the already electron-deficient $Ru_2{}^{4+}$ core.

It would appear that even relatively weak π-acceptor ligands such as MeCN or pyridine are capable of delocalising electron density, not only from the antibonding h.o.m.o.s, but also from the metal–metal bonding orbitals of the correct symmetry which lie just slightly lower in energy, which causes weakening of the bond. No evidence for equatorial (class II) 2:1 adduct formation or axial–equatorial (class III) 2:1 or 4:1 adduct formation, as recently noted for Mo and Rh compounds,[16,36,47] has been observed for $Ru_2(\mu\text{-}O_2CR)_4$ (R = Me or CF_3). However, the intermediacy of such adducts in the formation of monomers through metal–metal bond fission seems likely.

The reaction of $Ru_2(\mu\text{-}O_2CR)_4$ (R = Me or CF_3) with the strong π-acceptor NO to give the class I complexes $Ru_2(\mu\text{-}O_2CR)_4(NO)_2$, which contain a Ru–Ru single bond, is obviously anomalous. There must be a very strong (σ + π) interaction between the paramagnetic $Ru_2{}^{4+}$ core (two unpaired electrons) and NO aided by the similarity in energy of the metal *d* orbitals and the π* orbitals of NO. Such an axial interaction must significantly perturb the molecular orbital scheme of Norman *et al.*[11] for $Ru_2(\mu\text{-}O_2CH)_4$ which will now be required to account for such features as the diamagnetism and lowered metal–metal bond multiplicity of $Ru_2(\mu\text{-}O_2CR)_4(NO)_2$.

The complex $Ru_2(\mu\text{-}N_3Ph_2)_4$, which we infer from its diamagnetism has a $\sigma^2\pi^4\delta^2\pi^{*4}$ electronic configuration, has a different reactivity from $Ru_2(\mu\text{-}O_2CR)_4$ toward donors, reacting with NO or CO to form strong bis adducts and with the bulkier Bu^tNC to form a mono adduct. All three complexes are almost certainly class I adducts.

These observations suggest that electron density is delocalised essentially from the metal–metal antibonding h.o.m.o.s with little or no involvement from metal–metal bonding orbitals of the correct symmetry, which must, in contrast to the situation prevailing for $Ru_2(\mu\text{-}O_2CR)_4$, be of considerably lower energy.

No reaction is observed between $Ru_2(\mu\text{-}N_3Ph_2)_4$ and either pyridine or PPh_3. The lack of reactivity is almost certainly due to the steric constraints imposed by the bulky phenyl groups of the triazenido ligands.

Experimental

Microanalyses were by Imperial College and Pascher Laboratories, Bonn. Melting points were determined in sealed capillaries and are uncorrected. Infrared spectra were recorded in the region 4 000—200 cm^{-1} on a Perkin-Elmer 683 grating spectrometer in Voltalef 3S mulls unless otherwise stated. Mass spectra were obtained on a VG7070 spectrometer. Magnetic measurements (295 K) were made on an Evans balance (solid) and in 2% hexamethyldisiloxane–thf solution (305 K) by the Evans n.m.r. method. N.m.r. spectra were recorded on a JEOL FX90Q spectrometer. Electronic spectra were obtained on a Perkin-Elmer 551 spectrophotometer and e.s.r. spectra on a Varian E12 (*X*-band) spectrometer with 100-kHz magnetic field modulation. Electrochemical studies employed an E.G. and G. PAR model 174A polarographic analyser and 0.2 mol dm^{-3} $NBu^n{}_4PF_6$ solutions in thf, MeCN, Me_2CO, or CH_2Cl_2, or 0.1 mol dm^{-3} $NaPF_6$ or NaCl in water, at ambient temperature, with platinum working and auxiliary electrodes and a saturated calomel electrode (s.c.e.) reference electrode (against which ferrocene is oxidised at $E_{\frac{1}{2}}$ = +0.34 V). Scan rates of 20—500 mV s^{-1} were employed on all cyclic voltammetric studies. Conductivities were determined on a Data Scientific PTI-18 instrument.

All operations were carried out under purified argon. Solvents were dried conventionally then distilled and degassed before use. Nitric oxide (British Oxygen Co. cylinders, 0.35% NO_2) was passed through a steel cylinder packed with

powdered sodium hydroxide, and then through a copper spiral at −78 °C. The formate $Ru_2(\mu\text{-}O_2CH)_4$ was prepared as before.[5]

Preparations.—*Tetra-μ-acetato-diruthenium*(II,II)–*bis(tetrahydrofuran)*. $Ru_2(\mu\text{-}O_2CH)_4$ (1.50 g) was heated under reflux for 20 min in degassed MeOH (40 cm^3) containing lithium acetate (2.40 g). The red-brown solution containing an orange microcrystalline product was allowed to cool to ambient temperature, filtered off and the solid recrystallised from thf at −20 °C as large red-brown crystals. Yield: 2.10 g (92%).

Analogous products were obtained by employing $Na[O_2CR]$ (R = Et, Ph, or CH_2Cl) instead of $Li[O_2CMe]$. The R = CH_2Cl and Ph products were recrystallised from tetrahydrofuran at −20 °C in yields of 68% and 87% respectively; the propionate was recrystallised from Me_2CO at −20 °C in 73% yield.

catena-*Tetra-μ-acetato-(μ-trifluoroacetato-O,O′)-diruthenium*(II,III). $Ru_2(\mu\text{-}O_2CMe)_4$ (0.30 g) was heated under reflux in degassed MeOH (40 cm^3) in the presence of $Ag[O_2CCF_3]$ (1.82 g) to rapidly generate a deep red solution and a grey precipitate of metallic silver. After heating for 3 h the solution was filtered hot, evaporated to dryness, and the product recrystallised from thf at −20 °C as red-orange needles and dried *in vacuo* at 20 °C. Yield: 0.31 g (82%); m.p. 240 °C (decomp.); $\mu_{eff.}$ = 2.9 B.M. per Ru (solid and solution).

catena-*Tetra-μ-propionato-(μ-propionato-O,O′)-diruthenium*(II,III). $Ru_2(\mu\text{-}O_2CMe)_4$ (0.30 g) was heated under reflux in degassed propionic acid–propionic anhydride (9:1, 20 cm^3) to give a deep red solution which on cooling to room temperature deposited the red-brown microcrystalline product, which was collected, washed with Et_2O (2 × 30 cm^3), and dried *in vacuo* at 20 °C. Yield: 0.37 g (95%); m.p. 260 °C (decomp.); $\mu_{eff.}$ = 2.9 B.M. per Ru (solid and solution).

Tri-potassium and -sodium tetra-μ-carbonato-diruthenate(II,III) *hexahydrate*. $Ru_2(\mu\text{-}O_2CMe)_4$ (1.50 g), suspended in degassed water (200 cm^3) containing K_2CO_3 (4.00 g), was heated under reflux for 2 h to yield a bright red-orange solution and ruthenium metal as a grey solid. The solution was filtered hot and then evaporated. The orange powder was washed with water until it just began to dissolve, thus removing excess carbonate. The solid was then washed with MeOH (3 × 20 cm^3) and Et_2O (3 × 20 cm^3) and air dried. Yield: 1.75 g (77%); m.p. 250 °C (darkens); conductivity (H_2O): Λ_M = 315 ohm^{-1} cm^2 mol^{-1}.

$\{K_3[Ru_2(\mu\text{-}O_2CO)_4]\cdot 6H_2O\}_n$ (0.4 g) in degassed water (200 cm^3) was passed through a column of Amberlite CG-120 resin (type II, 200 mesh, Na^+ form). The bright orange solution was evaporated and the orange microcrystals washed with MeOH (3 × 20 cm^3) and Et_2O (3 × 20 cm^3) and air dried. Yield: 0.35 g (94%); m.p. 250 °C (darkens); conductivity (H_2O): Λ_M = 334 ohm^{-1} cm^2 mol^{-1}; $\mu_{eff.}$ = 2.9 B.M. per Ru (solid).

catena-*Tetra-μ-trifluoroacetato-(μ-trifluoroacetato-O,O′)-diruthenium*(II,III). $\{K_3[Ru_2(\mu\text{-}O_2CO)_4]\cdot 6H_2O\}_n$ (1.50 g) was suspended in non-degassed trifluoroacetic acid–trifluoroacetic anhydride (9:1, 30 cm^3) and stirred in air at ambient temperature. Dissolution of the salt, which was accompanied by evolution of CO_2, was complete within 10 min to give a bright orange solution which deposited a microcrystalline precipitate. After 12 h the solid was collected, washed with CF_3CO_2H (6 × 10 cm^3) and toluene (4 × 30 cm^3) and dried *in vacuo* at 20 °C. Yield: 1.54 g (89%); m.p. 190 °C (darkens); $\mu_{eff.}$ = 2.9 B.M. per Ru (solid).

Tetra-μ-trifluoroacetato-diruthenium(II,II)–*bis(tetrahydrofuran)*. *Method 1*. $\{K_3[Ru_2(\mu\text{-}O_2CO)_4]\cdot 6H_2O\}_n$ (1.50 g), suspended in degassed trifluoroacetic acid–trifluoroacetic anhydride (9:1, 30 cm^3) and Et_2O (10 cm^3), was stirred at ambient temperature under H_2 (7 atm) in a Fisher-Porter pressure bottle. The bright orange microcrystalline precipitate initially produced slowly redissolved to yield a deep red solution. After 24 h the deep red solution was filtered and evaporated. The orange solid was extracted into Et_2O which was then removed and the solid crystallised from thf–hexane as large deep red crystals which were dried *in vacuo* at 20 °C. Yield: 1.34 g (75%).

Method 2. $Ru_2(\mu\text{-}O_2CMe)_4$ (1.50 g) was heated under reflux in degassed trifluoroacetic acid–trifluoroacetic anhydride (9:1, 60 cm^3) containing $Na[O_2CCF_3]$ (2.80 g) for 72 h. The deep red solution was evaporated to dryness and worked-up as above. Yield: 1.48 g (54%); m.p. 240 °C (decomp.); mass spectrum: *m/e* 654, $[Ru_2(O_2CCF_3)_4]^+$; $\mu_{eff.}$ = 2.1 B.M. per Ru (solid and solution).

Tetra-μ-trifluoroacetato-diruthenium(II,II). $Ru_2(\mu\text{-}O_2CCF_3)_4(thf)_2$ (0.20 g) was heated at 150 °C under 0.1 mmHg pressure for 15 min; *ca.* 0.05 g of the volatile solvate sublimed on to a probe, leaving the much less volatile non-solvated complex as an orange powder. Yield: 0.11 g (67%); m.p. 240 °C (decomp.), mass spectrum: *m/e* 654, $[Ru_2(O_2CCF_3)_4]^+$; $\mu_{eff.}$ = 2.1 B.M. per Ru (solid).

Tetra-μ-acetato-bis(nitrosyl)diruthenium. $Ru_2(\mu\text{-}O_2CMe)_4$ (0.40 g) in thf (50 cm^3) was stirred for 30 min at ambient temperature under NO (1 atm). The orange-brown solution rapidly became orange-red and precipitated orange microcrystals which were collected and dried *in vacuo*. Yield: 0.41 g (90%); m.p. 280 °C (decomp.); mass spectrum: *m/e* 498, $[Ru_2(O_2CMe)_4(NO)_2]^+$.

Tetra-μ-benzoato-bis(nitrosyl)diruthenium. As above but with $Ru_2(\mu\text{-}O_2CPh)_4$ (0.40 g). Yield: 0.42 g (97%); m.p. 220 °C (decomp.); mass spectrum: *m/e* 746, $[Ru_2(O_2CPh)_4(NO)_2]^+$.

Bis(nitrosyl)tetra-μ-propionato-diruthenium. $Ru_2(\mu\text{-}O_2CEt)_4$ (0.40 g) in thf (40 cm^3) was exposed to NO (0.5 atm) for 5 min. The solution was evaporated and the residue recrystallised from hexane at −20 °C as large red prisms which were dried *in vacuo*. Yield: 0.37 g (83%); m.p. 120 °C; mass spectrum: *m/e* 554, $[Ru_2(O_2CEt)_4(NO)_2]^+$.

Bis(nitrosyl)tetra-μ-trifluoroacetato-diruthenium. As for the propionate but using $Ru_2(\mu\text{-}O_2CCF_3)_4$ (0.20 g) in Et_2O (20 cm^3). Yield: 0.15 g (69%); m.p. *ca.* 100 °C (decomp.); mass spectrum: *m/e* 714, $[Ru_2(O_2CCF_3)_4(NO)_2]^+$.

trans-*Diacetatotetrakis(t-butyl isocyanide)ruthenium*(II). $Ru_2(\mu\text{-}O_2CMe)_4$ (0.30 g), suspended in MeOH–Et_2O (1:1) (20 cm^3) containing excess Bu^tNC (1.0 cm^3), was stirred for 12 h. The pale yellow solution was evaporated and the residue recrystallised from Et_2O at −20 °C as white prisms which were dried *in vacuo*. Yield: 0.70 g (93%); m.p. 147 °C.

cis-*Tetrakis(t-butyl isocyanide)bis(trifluoroacetato)ruthenium*(II). $Ru_2(\mu\text{-}O_2CCF_3)_4(thf)_2$ (0.30 g) and Bu^tCN (0.8 cm^3) in n-hexane (50 cm^3) was stirred for 12 h. The white microcrystalline precipitate was collected, washed with n-hexane (2 × 10 cm^3), and dried *in vacuo*. Yield: 0.39 g (79%); m.p. 150 °C.

fac-*Tricarbonyl(tetrahydrofuran)bis(trifluoroacetato)ruthenium*(II). $Ru_2(\mu\text{-}O_2CCF_3)_4(thf)_2$ (0.30 g) in n-hexane (50 cm^3) was stirred for 18 h under CO (3.5 atm). The off-white solid was collected, dried, and recrystallised from thf–hexane at −20 °C as white microcrystals which were dried *in vacuo*. Yield: 0.28 g (77%); m.p. 80 °C; mass spectrum: *m/e* 411, $[Ru(O_2CCF_3)_2(CO)_3]^+$.

Diacetatobis(triphenylphosphine)ruthenium(II). $Ru_2(\mu\text{-}O_2CMe)_4$ (0.40 g) in MeOH (20 cm^3) was stirred for 24 h with two equivalents of PPh_3 (0.48 g). The orange-brown precipitate is the MeOH solvate of the starting material (43% yield). The orange solution was evaporated and the solid recrystallised from Me_2CO–Et_2O at −20 °C as orange microcrystals which were dried *in vacuo*. Yield: 0.57 g (42%); m.p. 189 °C (decomp.).

Bis(trifluoroacetato)bis(triphenylphosphine)ruthenium(II). $Ru_2(\mu\text{-}O_2CCF_3)_4$ (0.30 g) suspended in MeOH (15 cm^3) was stirred for 24 h with two equivalents of PPh_3 (0.24 g). After

Table 9. Crystallographic data

(*a*) Crystal data				
Complex	$Ru_2(\mu\text{-}O_2CCF_3)_4(thf)_2$	$\{Na_3[Ru_2(\mu\text{-}O_2CO)_4]\cdot 6H_2O\}_n$	$Ru_2(\mu\text{-}O_2CEt)_4(NO)_2$	$Ru_2(\mu\text{-}O_2CCF_3)_4(NO)_2$
Formula	$C_{16}H_{16}F_{12}O_{10}Ru_2$	$C_4H_{12}Na_3O_{18}Ru_2$	$C_{12}H_{20}N_2O_{10}Ru_2$	$C_8F_{12}N_2O_{10}Ru_2$
M	798.417	619.237	554.437	714.214
a/Å	8.739(3)	9.485(3)	9.746(3)	9.299(1)
b/Å	9.434(4)	9.610(2)	13.007(3)	15.034(2)
c/Å	9.737(4)	9.896(2)	8.173(5)	13.498(2)
α/°	117.72(3)	110.38(2)	90	90
β/°	73.58(3)	72.02(2)	106.86(3)	91.69(2)
γ/°	106.55(3)	92.35(2)	90	90
U/Å^3	670.43(50)	802.03(38)	991.53(73)	1 872.02(42)
System	Triclinic	Triclinic	Monoclinic	Monoclinic
Space group	$P\bar{1}$	$P\bar{1}$	$P2_1/a$	$C2/c$
D_c/g cm^{-3}	1.98	2.564	1.86	2.54
Z	1	2	2	4
$F(000)$	388	602	548	1 352
μ(Mo-K_α)/cm^{-1}	12.30	20.19	15.42	17.50
(*b*) Data collection				
$\theta_{min.,max.}$/°	1.5, 25	1.5, 23	1.5, 25	1.5, 23
Total data measured	2 445	2 502	2 001	1 870
Total unique data	2 358	2 394	1 739	1 646
Total data observed	2 020	1 650	1 184	1 156
Significance test	$F_o > 4\sigma(F_o)$	$F_o > 3\sigma(F_o)$	$F_o > 4\sigma(F_o)$	$F_o > 4\sigma(F_o)$
(*c*) Refinement				
No. of parameters	213	290	158	172
Weighting scheme parameter g[a]	0.000 01	0.000 01	0.000 01	0.000 02
Final R[b]	0.0389	0.0340	0.0261	0.0346
Final R'[c]	0.0444	0.0299	0.0290	0.0350

[a] $w = 1/[\sigma^2(F_o) + gF_o^2]$. [b] $R = \sum(\Delta F)/\sum(F_o)$. [c] $R' = [\sum w(\Delta F)^2/\sum w(F_o^2)]^{\frac{1}{2}}$.

Table 10. Fractional atomic co-ordinates ($\times 10^4$) for $Ru_2(\mu\text{-}O_2CCF_3)_4(thf)_2$

Atom	x	y	z
Ru(1)	−560(1)	−231(1)	6 101(1)
O(1)	638(5)	2 039(5)	7 446(5)
O(2)	−1 728(5)	−2 500(4)	4 713(5)
O(3)	1 369(5)	−1 331(5)	5 694(5)
O(4)	−2 469(5)	874(5)	6 475(5)
O(5)	−1 659(7)	−745(5)	8 266(5)
C(1)	1 449(8)	2 884(7)	6 728(8)
C(2)	2 162(10)	4 635(8)	7 752(9)
C(3)	−2 388(8)	1 430(7)	5 519(8)
C(4)	−3 702(10)	2 394(9)	5 892(10)
C(5)	−2 188(13)	382(11)	9 755(10)
C(6)	−3 031(14)	−477(15)	10 721(11)
C(7)	−3 246(16)	−2 149(13)	9 668(12)
C(8)	−2 316(16)	−2 298(10)	8 234(11)
F(1)	2 421(9)	4 836(6)	9 036(7)
F(2)	1 226(8)	5 573(6)	8 022(9)
F(3)	3 513(7)	5 177(6)	7 038(7)
F(4)	−3 867(9)	2 561(11)	4 746(9)
F(5)	−3 419(9)	3 779(7)	6 980(11)
F(6)	−5 130(6)	1 747(7)	6 377(8)

cooling to −20 °C, the red-orange solution was filtered from a yellow precipitate which was collected, washed with hexane (2 × 10 cm^3), and dried *in vacuo* at 20 °C. Yield: 0.28 g (36%); m.p. 194 °C (decomp.). The solution contained $Ru_2(\mu\text{-}O_2CCF_3)_4(thf)_2$ (37% yield) which was recovered.

Pentakis(acetonitrile)trifluoroacetatoruthenium(II) *trifluoroacetate*. $Ru_2(\mu\text{-}O_2CCF_3)_4$ (0.40 g) in MeCN (50 cm^3) is initially orange-red becoming paler on stirring. Although the solution was almost colourless within 10 min the reaction was allowed to

Table 11. Fractional atomic co-ordinates ($\times 10^4$) for $\{Na_3[Ru_2(\mu\text{-}O_2CO)_4]\cdot 6H_2O\}_n$

Atom	x	y	z
Ru(1)	389(1)	1 133(1)	501(1)
Ru(2)	4 428(1)	−4 035(1)	−71(1)
Na(1)	3 772(4)	1 595(4)	1 997(4)
Na(2)	5 000*	0*	5 000*
Na(3)	−64(4)	5 996(5)	3 829(5)
Na(4)	−299(9)	4 457(9)	58(10)
O(11)	1 478(6)	1 128(6)	−1 599(6)
O(12)	2 238(5)	124(6)	461(6)
O(13)	−697(6)	1 136(6)	2 624(6)
O(14)	−1 446(6)	2 123(6)	494(6)
O(15)	2 085(6)	31(7)	−4 108(6)
O(16)	3 672(6)	−1 883(6)	−126(6)
O(21)	4 346(6)	−2 840(6)	2 081(6)
O(22)	4 454(6)	−5 263(6)	−2 204(6)
O(23)	6 443(5)	−3 295(6)	−836(6)
O(24)	2 414(5)	−4 769(6)	709(6)
O(25)	4 988(7)	−2 583(6)	4 130(6)
O(26)	1 080(6)	−6 475(6)	1 428(6)
O(01)	5 198(10)	−25(9)	2 463(8)
O(02)	−4 151(8)	6 308(9)	5 985(8)
O(03)	1 601(8)	1 763(9)	4 096(8)
O(04)	−1 493(9)	6 268(10)	2 348(10)
O(05)	−1 203(8)	1 889(9)	−3 439(9)
O(06)	−1 591(10)	4 349(12)	4 875(10)
C(1)	1 437(9)	−20(10)	−2 824(9)
C(2)	2 467(9)	−1 312(9)	−47(7)
C(3)	4 959(9)	−3 369(9)	2 847(9)
C(4)	2 356(9)	−6 014(9)	990(9)

* Invariant parameter.

Table 12. Fractional atomic co-ordinates ($\times 10^4$) for $Ru_2(\mu\text{-}O_2CR)_4(NO)_2$ (R = Et or CF_3)

R = Et				R = CF_3*			
Atom	*x*	*y*	*z*	Atom	*x*	*y*	*z*
Ru(1)	6 291(0.5)	5 024(0.5)	888(1)	Ru(1)	3 340(1)	3 086(0.5)	5 368(0.5)
O(1)	6 025(4)	3 560(3)	1 662(5)	O(1)	5 005(6)	2 298(4)	4 888(4)
O(2)	6 281(4)	6 467(3)	−144(5)	O(2)	3 237(6)	3 676(4)	3 989(4)
O(3)	6 857(4)	4 402(3)	−1 117(5)	O(3)	1 485(6)	3 734(4)	5 760(4)
O(4)	5 422(4)	5 620(3)	2 709(4)	O(4)	3 263(6)	2 361(4)	6 660(4)
N(1)	7 972(5)	5 305(4)	2 400(6)	N(1)	4 595(20)	3 742(14)	6 167(15)
O(5)	8 671(6)	5 746(7)	3 519(10)	N(1′)	4 388(20)	4 049(12)	5 685(15)
C(1)	4 817(6)	3 130(4)	1 127(7)	O(11)	5 162(19)	3 887(13)	6 881(13)
C(2)	4 678(8)	2 052(5)	1 735(9)	O(11′)	4 808(23)	4 733(12)	5 525(18)
C(3)	5 833(12)	1 425(7)	1 920(22)	C(11)	4 723(9)	1 586(6)	4 450(6)
C(4)	5 884(6)	4 203(4)	−2 467(7)	C(12)	6 026(11)	1 084(8)	4 083(8)
C(5)	6 298(8)	3 729(6)	−3 931(9)	C(21)	2 494(9)	3 320(6)	3 315(6)
C(6)	7 763(9)	3 379(7)	−3 609(10)	C(22)	2 516(12)	3 775(7)	2 286(7)
				F(11)	6 354(8)	1 316(6)	3 213(5)
				F(12)	7 134(9)	1 153(9)	4 627(6)
				F(13)	5 767(10)	244(6)	3 986(8)
				F(21)	2 895(10)	4 598(5)	2 359(5)
				F(22)	1 349(9)	3 735(8)	1 824(6)
				F(23)	3 514(10)	3 420(6)	1 775(5)

*See text.

continue for 40 h. The solution was evaporated and the residue crystallised from MeCN–Et_2O at −20 °C to give white microcrystals which were dried *in vacuo*. Yield: 0.55 g (85%); m.p. 140 °C (decomp.); conductivity (MeCN): Λ_M = 133 ohm^{-1} cm^2 mol^{-1}.

trans-*Diacetatotetrakis(pyridine)ruthenium*(II). $Ru_2(\mu\text{-}O_2CMe)_4$ (0.30 g) in MeOH (50 cm^3) and excess pyridine (2.0 cm^3) was stirred for 18 h. The yellow-orange solution was evaporated and the residue washed with cold Me_2CO (4 × 10 cm^3) to remove small quantities of $Ru(O_2CMe)_2(py)_2$ impurity. The residual solid was crystallised at −20 °C from CH_2Cl_2–hexane as orange–red prisms. Yield: 0.61 g (83%); m.p. 210 °C (decomp.).

trans-*Tetrakis(pyridine)bis(trifluoroacetato)ruthenium*(II). $Ru_2(\mu\text{-}O_2CCF_3)_4$ (0.30 g) in Et_2O (10 cm^3) and excess pyridine (2.0 cm^3) were stirred for 18 h. The yellow precipitate was separated from a green-orange solution and recrystallised from CH_2Cl_2–hexane at −20 °C as orange-yellow crystals which were dried *in vacuo*. Yield: 0.42 g (71%); m.p. 185 °C.

Tetra-μ-diphenyltriazenido-diruthenium(II,II). $Ru_2(\mu\text{-}O_2CMe)_4$ (1.50 g) in Et_2O (200 cm^3) was treated with four equivalents of $Li[N_3Ph_2]$ in Et_2O (50 cm^3) and stirred for 18 h. The deep red solution was evaporated to give a dark residue which was washed with MeOH (10 × 30 cm^3) until the washings were pale pink. The red-purple solid was extracted into the minimum volume of hot toluene which on cooling at −20 °C gave deep red-purple microcrystals which were dried *in vacuo*. Yield: 1.47 g (44%); m.p. 220 °C (decomp.); mass spectrum: *m/e* 986, $[Ru_2(N_3Ph_2)_4]^+$.

Tetra-μ-diphenyltriazenido-bis(nitrosyl)diruthenium. $Ru_2(\mu\text{-}N_3Ph_2)_4$ (0.40 g) in CH_2Cl_2 (50 cm^3) was exposed for *ca.* 5 min to NO (0.5 atm). The red-orange solution was filtered, concentrated to approximately half volume, and cooled at −20 °C. The orange prismatic plates were collected, washed with hexane, and dried *in vacuo*. Yield: 0.35 g (83%); m.p. 140 °C, decomp. 220 °C; mass spectrum: *m/e* 986, $[Ru_2(N_3Ph_2)_4]^+$.

Tetra-μ-diphenyltriazenido-(t-butyl isocyanide)diruthenium-(II,II). $Ru_2(\mu\text{-}N_3Ph_2)_4$ (0.40 g) in toluene (50 cm^3) was stirred for 2 h with excess Bu^tNC (0.2 cm^3). The red-pink solution was evaporated and the solid crystallised from CH_2Cl_2–hexane as red needle plates and dried *in vacuo*. Yield: 0.37 g (85%); m.p. 220 °C (decomp.); mass spectrum: *m/e* 986, $[Ru_2(N_3Ph_2)_4]^+$.

Dicarbonyltetra-μ-diphenyltriazenido-diruthenium(II,II). $Ru_2(\mu\text{-}N_3Ph_2)_4$ (0.40 g) in toluene (50 cm^3) was stirred for 18 h under CO (2 atm) to give a purple-blue microcrystalline precipitate which was crystallised from CH_2Cl_2 at −20 °C as deep blue rectangular plates that were dried *in vacuo*. Yield: 0.33 g (78%); m.p. 220 °C (decomp.); mass spectrum: *m/e* 986, $[Ru_2(N_3Ph_2)_4]^+$.

Crystallography.—The crystals for *X*-ray study were sealed in thin-walled capillaries under argon. Measurements were made using a CAD4 diffractometer operating in the ω–2θ scan mode with graphite-monochromated Mo-K_α radiation (λ = 0.710 69 Å) as previously described.[48] The data were all corrected for absorption empirically. The structures were solved *via* the heavy-atom method and refined routinely by full-matrix least squares using SHELX.[49] In each case, except the carbonato complex, all hydrogens were located experimentally and freely refined isotropically; non-H atoms were refined anisotropically. In the trifluoroacetate-nitrosyl complex, the nitrosyl ligands are disordered over two sites with occupancies 0.47 [N(1),O(11)] and 0.53 [N(1′),O(11′)]. Scattering factor data were taken from ref. 50. Crystal data and details of intensity measurements and structure refinement are given in Table 9. Final atomic fractional co-ordinates are given in Tables 10–12.

Acknowledgements

We thank the S.E.R.C. for support and for provision of *X*-ray facilities, and Johnson Matthey plc for the loan of ruthenium.

References

1 F. A. Cotton and R. A. Walton, 'Multiple Bonds between Metal Atoms,' J. Wiley and Sons, New York, 1982.
2 F. A. Cotton and G. Wilkinson, 'Advanced Inorganic Chemistry,' 4th edn., J. Wiley and Sons, New York, 1980.
3 T. R. Felthouse, *Prog. Inorg. Chem.*, 1982, **29**, 73.
4 E. B. Boyer and S. D. Robinson, *Coord. Chem. Rev.*, 1983, **50**, 109.
5 A. J. Lindsay, M. Motevalli, M. B. Hursthouse, and G. Wilkinson, *J. Chem. Soc., Dalton Trans.*, 1985, 2321.
6 T. A. Stephenson and G. Wilkinson, *J. Inorg. Nucl. Chem.*, 1966, **28**, 2285.
7 F. A. Cotton and E. Pedersen, *Inorg. Chem.*, 1975, **14**, 388.
8 R. C. Mehrota and R. Bohra, 'Metal Carboxylates,' Academic Press, London, 1983.
9 T. Malinski, D. Chong, F. N. Feldmann, J. L. Bear, and K. M. Kadish, *Inorg. Chem.*, 1983, **22**, 3225.

10 M. Mukaida, T. Nomura, and T. Ishimori, *Bull. Chem. Soc. Jpn.*, 1972, **45**, 2143.
11 J. G. Norman, jun., G. E. Renzoni, and P. A. Case, *J. Am. Chem. Soc.*, 1979, **101**, 5256.
12 M. Berry, C. D. Garner, I. H. Hillier, A. A. MacDowell, and W. Clegg, *Inorg. Chim. Acta*, 1981, **53**, L61.
13 K. Das, K. M. Kadish, and J. L. Bear, *Inorg. Chem.*, 1978, **17**, 930.
14 V. Gutmann, *Electrochim. Acta*, 1976, **21**, 661.
15 R. R. Schrock, B. F. G. Johnson, and J. Lewis, *J. Chem. Soc., Dalton Trans.*, 1974, 951.
16 G. S. Girolami and R. A. Andersen, *Inorg. Chem.*, 1981, **20**, 2040.
17 R. Ouahes, H. Pezerat, and J. Gayoso, *Rev. Chim. Mineral.*, 1970, **7**, 849.
18 F. A. Cotton and G. W. Rice, *Inorg. Chem.*, 1978, **17**, 2004.
19 (*a*) F. A. Cotton and T. R. Felthouse, *Inorg. Chem.*, 1980, **19**, 320; (*b*) C. R. Wilson and H. Taube, *ibid.*, 1975, **14**, 405.
20 J. A. Valentine, D. Valentine, jun., and J. P. Collman, *Inorg. Chem.*, 1971, **10**, 219.
21 T. Kimura, T. Sakurai, M. Shima, T. Nagai, K. Mizumachi, and T. Ishimori, *Acta Crystallogr., Sect. B*, 1982, **38**, 112.
22 A. J. Lindsay, M. Motevalli, M. B. Hursthouse, and G. Wilkinson, *J. Chem. Soc., Chem. Commun.*, 1986, 433.
23 R. J. Angelici, 'Synthesis and Technique in Inorganic Chemistry,' 2nd edn., W. B. Saunders Company, Philadelphia, 1977.
24 K. Nakamoto, 'Infrared Spectra of Inorganic and Coordination Compounds,' 3rd edn., J. Wiley and Sons, New York, 1978.
25 F. A. Cotton, M. W. Extine, and G. W. Rice, *Inorg. Chem.*, 1978, **17**, 176.
26 F. A. Cotton, G. W. Rice, and J. C. Sekutowski, *Inorg. Chem.*, 1979, **18**, 1143.
27 J. A. Edgar, Ph.D. Thesis, University of Minnesota, 1971.
28 K. R. Laing, S. D. Robinson, and M. F. Uttley, *J. Chem. Soc., Dalton Trans.*, 1974, 1205; C. J. Creswell, M. A. M. Queiros, and S. D. Robinson, *Inorg. Chim. Acta*, 1982, **60**, 157; W. H. Knoth, *Inorg. Chem.*, 1973, **12**, 38; L. D. Brown and J. A. Ibers, *ibid.*, 1976, **15**, 2788.
29 J. P. Collman, C. E. Barnes, T. J. Collins, P. J. Brothers, J. Gallucci, and J. A. Ibers, *J. Am. Chem. Soc.*, 1981, **103**, 7030; J. P. Collman, C. E. Barnes, P. N. Swepston, and J. A. Ibers, *ibid.*, 1984, **106**, 3500.
30 P. I. van Vliet, J. Kuyper, and K. Vrieze, *J. Organomet. Chem.*, 1976, **105**, 379; 1976, **122**, 99; E. Pfeffer, A. Oskam, and K. Vrieze, *Transition Met. Chem. (Weinheim, Ger.)*, 1977, **2**, 240; R. Rossi, A. Quatti, L. Magon, U. Casellato, R. Graziani, and L. Tonido, *J. Chem. Soc., Dalton Trans.*, 1982, 1949.
31 D. J. Santure, J. C. Huffman, and A. P. Sattelberger, *Inorg. Chem.*, 1985, **24**, 371.
32 B. L. Haymore and J. A. Ibers, *Inorg. Chem.*, 1975, **14**, 3060.
33 J. H. Enemark and R. D. Feltham, *Coord. Chem. Rev.*, 1974, **13**, 339.
34 R. D. Feltham and J. H. Enemark, 'Topics in Inorganic and Organometallic Stereochemistry,' ed. G. L. Geoffroy, Wiley-Interscience, New York, 1981.
35 R. Eisenberg, A. P. Graham, jun., C. G. Pierpont, J. Read, and A. J. Shultz, *J. Am. Chem. Soc.*, 1972, **94**, 6240.
36 G. S. Girolami, V. V. Mainz, and R. A. Andersen, *Inorg. Chem.*, 1980, **19**, 805.
37 K. Teramoto, Y. Sasaki, K. Migita, M. Iwaizumi, and K. Saito, *Bull. Chem. Soc. Jpn.*, 1979, **52**, 446.
38 C. M. Mitchell and F. G. A. Stone, *J. Chem. Soc., Dalton Trans.*, 1972, 102; R. B. King and R. N. Kapoor, *J. Organomet. Chem.*, 1968, **15**, 457; A. Dobson and S. D. Robinson, *Inorg. Chem.*, 1977, **16**, 1321.
39 R. S. Drago, S. P. Tanner, R. M. Richman, and J. R. Long, *J. Am. Chem. Soc.*, 1979, **101**, 2897.
40 L. Malatesta, G. A. Padoa, and A. Sonz, *Gazz. Chim. Ital.*, 1955, **85**, 1111; B. E. Prater, *J. Organomet. Chem.*, 1971, **33**, 215.
41 Y. Yamamoto, H. Aoki, and H. Yamazaki, *Inorg. Chem.*, 1979, **18**, 1681.
42 R. A. Walton, 'Reactivity of Metal–Metal bonds,' ed. M. H. Chisholm, *ACS Symp. Ser.*, No. 155, American Chemical Society, Washington D.C., 1981.
43 G. C. Christoph and Y. B. Koh, *J. Am. Chem. Soc.*, 1979, **101**, 1422.
44 E. A. Seddon and K. R. Seddon, 'The Chemistry of Ruthenium,' Elsevier, Amsterdam, 1984.
45 M. I. Bruce and F. G. A. Stone, *J. Chem. Soc. A*, 1967, 1238; B. F. G. Johnson, R. D. Johnston, and J. Lewis, *ibid.*, 1969, 792.
46 J. D. Gilbert and G. Wilkinson, *J. Chem. Soc. A*, 1969, 1749; R. A. Sanchez-Delgado, J. S. Bradley, and G. Wilkinson, *J. Chem. Soc., Dalton Trans.*, 1976, 399.
47 J. Telser and R. S. Drago, *Inorg. Chem.*, 1986, **25**, 2989; 1984, **23**, 2599.
48 M. B. Hursthouse, R. A. Jones, K. M. A. Malik, and G. Wilkinson, *J. Am. Chem. Soc.*, 1979, **101**, 4128.
49 G. M. Sheldrick, SHELX 76, University of Cambridge, 1976.
50 'International Tables for *X*-Ray Crystallography,' Kynoch Press, Birmingham, 1974, vol. 4.

Received 17*th November* 1986; *Paper* 6/2213